The Coordination Chemistry of *cis*-3,4-Diaminopyrrolidine and Related Polyamines[‡]

Dirk Kuppert,[a] Jürgen Sander,[a] Christian Roth,[a] Michael Wörle,[b] Thomas Weyhermüller,[c] Guido J. Reiss,[d] Uwe Schilde,[e] Iris Müller,[f] and Kaspar Hegetschweiler*[a]

Keywords: Chelates / N ligands / Ligand design / Stability constants / Coordination modes

cis-3,4-Diaminopyrrolidine (*cis*-dap), *trans*-3,4-diaminopyrrolidine (*trans*-dap), *cis*-1,2-cyclopentanediamine (*cis*-cptn), and *trans*-1,2-cyclopentanediamine (*trans*-cptn) have been prepared in multigram quantities. The complexation of these ligands and of 3-aminopyrrolidine (ampy) with Ni^{II}, Cu^{II}, Zn^{II}, and Cd^{II} has been studied in solution by means of potentiometric and spectrophotometric titrations. The complexes of the triamines *cis*-dap and *trans*-dap show a pronounced tendency to form protonated species such as $[M^{II}(HL)]^{3+}$, $[M^{II}(HL)_2]^{4+}$, and $[M^{II}(HL)L]^{3+}$, indicative of a bidentate coordination mode of the ligand L. The UV/Vis spectra of the corresponding Cu^{II} complexes further confirmed bidentate coordination with *trans*-CuN_4 geometry. The overall stabilities of the bis complexes $[ML_2]^{2+}$ decrease in the order *cis*-cptn > *cis*-dap > *trans*-cptn > ampy > *trans*-dap. The considerably lower stabilities of the ampy complexes as compared to the corresponding *cis*-dap complexes indicate metal binding to the two primary amino groups of the latter ligand. This was supported by molecular mechanics calculations (Cu^{II} and Co^{III} complexes) and confirmed by single-crystal X-ray diffraction studies of $[Pt(Hcis\text{-}dap)Cl_4]Cl\cdot H_2O$, $[Pd(Hcis\text{-}dap)_2](ClO_4)_4\cdot 2H_2O$, and $[Cu(Hcis\text{-}dap)_2(OH_2)_2](SO_4)_2\cdot 3.5H_2O$ – $2x\ H^+ + x\ Cu^{2+}$ with $0.01 \le x \le 0.11$. For the diamine ligands, coordination through the two exocyclic amino groups or through one exocyclic and one endocyclic amino group was established from the X-ray structure analyses of $[Ni(cis\text{-}cptn)_2](ClO_4)_2$ and $[Cu(3R\text{-}ampy)(3S\text{-}ampy)](ClO_4)_2$, respectively. The crystal structure determination of $[Co(cis\text{-}dap)(tach)][ZnCl_4]Cl\cdot C_2H_5OH$ (tach = *cis*-1,3,5-cyclohexanetriamine) revealed tridentate, facial coordination of *cis*-dap in this particular complex. However, the structural parameters of the $[Co(cis\text{-}dap)(tach)]^{3+}$ moiety indicate significant strain for this coordination mode. The coordinating properties of the ligand *cis*-dap are compared with those of other aliphatic and alicyclic triamines.

Introduction

Structure–stability correlations are a subject of continuing interest in coordination chemistry, and the dependence of complex stability on the individual structural properties of a ligand has been extensively discussed.[1] In this respect, cyclic polyamines that are restricted to a facial coordination (Scheme 1) are of particular interest because their rigidity considerably reduces the number of possible solution structures as compared to their open-chain analogues. Ligands based on the 1,4,7-triazacyclononane or all-*cis*-cyclohexane-1,3,5-triamine backbone are well established in the literature.[2,3] However, until recently, intermediate members of this series, such as *cis*-3,5-diaminopiperidine (dapi) or *cis*-3,4-diaminopyrrolidine (*cis*-dap), had not been investigated to any great extent. Crystal structures of Pd^{II}(dapi) complexes have been reported by Schwarzenbach,[4] and we recently published a comprehensive study of the complexation of dapi with a variety of metal cations.[5] The metal-binding properties of the related triamine *cis*-3,4-diaminopyrrolidine (*cis*-dap) have not yet been described. We have developed an efficient procedure for the preparation of *cis*-dap and wish to report herein its coordination chemistry both in aqueous solution and in the solid state. Additionally, some related cyclic di- and triamine ligands with a five-membered ring structure have also been studied (Scheme 2).

Results

Synthesis of the Ligands

The only hitherto known synthesis of *cis*-3,4-diaminopyrrolidine involves a complicated multi-step procedure and gives only unsatisfactory yields.[6] We have developed a new and efficient synthetic route that has allowed facile

[‡] Facially Coordinating Cyclic Triamines, 2. – Part 1: Ref.[5]
[a] Anorganische Chemie, Universität des Saarlandes, Postfach 151150, 66041 Saarbrücken, Germany
Fax: (internat.) + 49-(0)681/302-2663
E-mail: hegetschweiler@mx.uni-saarland.de
[b] Laboratorium für Anorganische Chemie, ETH-Zentrum, 8092 Zürich, Switzerland
[c] Max-Planck-Institut für Strahlenchemie, Stiftstraße 34–36, 45470 Mühlheim an der Ruhr, Germany
[d] Institut für Anorganische Chemie und Strukturchemie, Heinrich-Heine-Universität Düsseldorf, Universitätsstraße 1, 40225 Düsseldorf, Germany
[e] Institut für Anorganische Chemie und Didaktik der Chemie, Universität Potsdam, Karl-Liebknecht-Straße 24–25, 14476 Golm, Germany
[f] Institut für Analytische Chemie, Ruhr-Universität, 44780 Bochum, Germany
Supporting information for this article is available on the WWW under http://www.eurjic.com or from the author.

  1434–1948/01/1010–2525 $ 17.50+.50/0

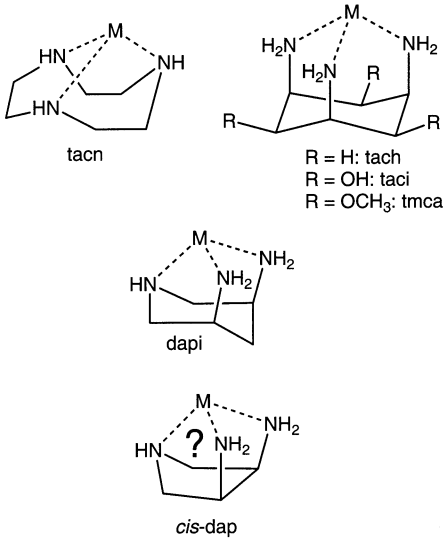

Scheme 1

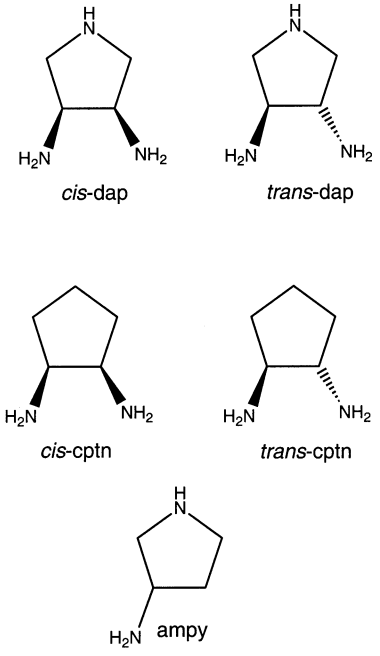

Scheme 2. Structures of the ligands and their abbreviations

preparation of this triamine in multigram quantities. Our procedure starts with 3-pyrroline, the amino group of which is protected by acetylation. The carbon−carbon double bond is then stereoselectively *cis*-dihydroxylated with OsO_4 to give 1-acetyl-*cis*-3,4-pyrrolidinediol. Subsequent conversion of the two hydroxy groups into amino groups is achieved through the corresponding diazide. After removal of the protecting acetyl group, the desired *cis*-3,4-diaminopyrrolidine can be isolated in excellent yield as the trihydrochloride salt. The *cis* configuration of the product was established by a single-crystal X-ray diffraction analysis (Figure 1, top). The corresponding chiral *trans* isomer was hitherto unknown and only some 1-substituted derivatives have been described.[7,8] We prepared this ligand from the *N*-benzylimide derivative of tartaric acid, which was again converted into the corresponding diazide. Subsequent hydrogenation resulted in reduction of the azido groups and in the removal of the benzyl group. The *trans* (3*R*,4*R*) configuration was again confirmed by a single-crystal X-ray diffraction analysis (Figure 1, bottom). The puckering parameters $Q = 0.405(2)$ Å, $\varphi = 83.0(4)°$ and $Q = 0.357(3)$ Å, $\varphi = 238.3(4)°$ for the pyrrolidine rings of H_3*cis*-dap^{3+} and H_3*trans*-dap^{3+} are indicative of a half-chair conformation with a slight twist towards an envelope form.[9] As expected, the N···N distance between the two primary amino groups in *trans*-dap is somewhat longer (3.28 Å) than that in *cis*-dap (3.00 Å).

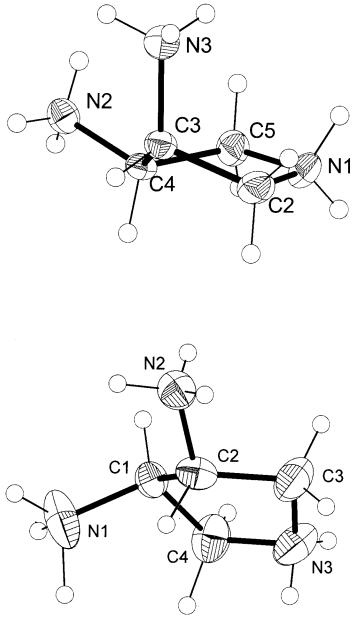

Figure 1. Molecular structures of the triply protonated triamines H_3*cis*-dap^{3+} (top) and H_3*trans*-dap^{3+} (bottom) showing the atom numbering scheme; thermal ellipsoids are drawn at a 50% probability level; hydrogen atoms are shown as spheres of arbitrary size; range of bond lengths [Å]: C−C 1.520(3)−1.533(3), C−N 1.478(3)−1.510(3); selected angles for H_3*cis*-dap^{3+} [°]: C2−C3−C4 100.93(16), N3−C3−C4 114.11(16), N2−C4−C3 116.80(17)

The structurally related diamines *cis*-1,2-cyclopentanediamine (*cis*-cptn) and *trans*-1,2-cyclopentanediamine (*trans*-cptn) were analogously prepared via the diazides using the corresponding cyclopentanediols as starting materials.[10−12] The chiral *trans*-cptn was obtained as a racemate. The two diastereomers can readily be distinguished by ^{1}H NMR spectroscopy. The *cis* isomer has C_s symmetry and shows four resonances due to the three methylene groups, whereas the chiral *trans* isomer exhibits C_2 symmetry showing only three signals for these six protons. The diamine 3-aminopyrrolidine (ampy) is commercially available and was again used as a racemate. A single-crystal X-ray diffraction analysis of H_2ampy$(ClO_4)_2$ has recently been published.[13]

Protonation Constants

The acidity constants of the protonated amines are listed in Table 1. For the two pairs of diastereomers H_3*cis*-dap^{3+}/H_3*trans*-dap^{3+} and H_2*cis*-cptn^{2+}/H_2*trans*-cptn^{2+}, the *cis* isomers of the fully protonated forms are slightly stronger acids. The triamines have different basic sites (primary and secondary amino groups) and this leads to different tautomers for species with an intermediate degree of protonation. In the case of *cis*-dap, the equilibria between these different microspecies were elucidated by ^{1}H NMR titration (Figure 2). An NOESY experiment allowed the unambiguous assignment of the two diastereotopic protons of the methylene groups. Only one proton (3-H) showed a significant NOE with the adjacent 1-H proton. The observed pH dependence of the chemical shifts could be reproduced using pK_a values of 2.15, 6.21, and 9.78 for the macrospecies H_x*cis*-dap^{x+} (Figure 2; $3 \geq x \geq 1$). These values (D_2O, 28 °C, no inert electrolyte) are in good agreement with the pK_a values obtained from the potentiometric measurements. As

Table 1. Protonation constants for the cyclic di- and triamine ligands (25 °C) at ionic strengths (I) of 0.1 mol dm^{-3} (KCl) and 1.0 mol dm^{-3} (KNO_3) as indicated

[a]	log K_1		log K_2		log K_3	
I [mol dm^{-3}]	0.1	1.0	0.1	1.0	0.1	1.0
ampy	10.39	10.66	6.82	7.20	–	–
cis-cptn	9.74	–	6.13	–	–	–
trans-cptn	9.92	–	7.22	–	–	–
cis-dap	9.66	9.90	6.25	6.63	2.42	2.96
trans-dap	9.58	9.80	6.34	6.72	3.67	4.19

[a] $K_i = [H_iL] \times [H]^{-1} \times [H_{i-1}L]^{-1}$; estimated standard deviations < 0.01.

described previously,[5] the deshielding of the (C−)H protons by protonation of a nearby basic site in a cyclic polyamine can be modeled using a limited set of deshielding constants. For the monoprotonated H*cis*-dap$^+$, such calcula-

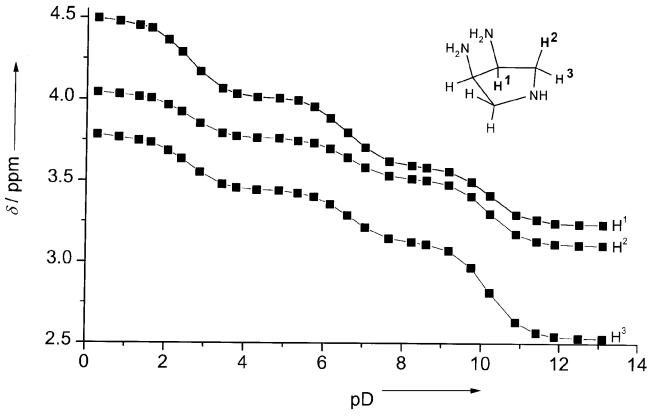

Figure 2. pD dependence of the ^{1}H NMR resonances of *cis*-dap; squares correspond to the experimental values; the lines are calculated (minimization of $[\delta_{obs} - \delta_{calcd.}]^2$) assuming a rapid equilibrium between the species H_x*cis*-dap^{x+} ($1 \leq x \leq 3$)

tions indicated that the two microspecies with a protonated primary amino group or a protonated secondary ring nitrogen atom are present in proportions of 57% and 43%, respectively. This ratio corresponds closely to a statistical distribution of the proton over the three basic sites. A different result is obtained for the doubly protonated H_2*cis*-dap^{2+}, for which the tautomer with a free primary amino group clearly predominates (75%). This result can be explained in terms of a simple electrostatic model (maximal separation of the two positive charges).

Metal Complex Formation

The coordination behavior of the polyamines in dilute aqueous solution (25 °C) was studied by means of pH-metric titration experiments. Formation constants of Ni^{II}, Cu^{II}, and Cd^{II} complexes were determined for ampy, *cis*-cptn, and *cis*-dap. Additionally, the complexation of *cis*-dap with Zn^{II} was studied. For the ligands *trans*-cptn and *trans*-dap, our study was confined to complexation with Cu^{II}. All formation constants are summarized in Tables 2 and 3. The measurements with Ni^{II}, Cu^{II}, and Zn^{II} were performed in 0.1 mol dm^{-3} KCl. Due to the relatively high affinity of Cd^{II} for Cl^-, these experiments were performed in 0.1 mol dm^{-3} KNO_3.[5]

Table 2. Formation constants of metal complexes with the triamine ligands (25 °C, 0.1 mol dm^{-3} KCl or KNO_3)

	Cu^{2+}		Ni^{2+}	Zn^{2+}	Cd^{2+}[a]
	cis-dap	*trans*-dap	*cis*-dap	*cis*-dap	*cis*-dap
log β_{xyz}[b] x,y,z					
1,1,0	–	–	6.41(1)	4.93(2)	4.44(2)
1,1,1	16.8(1)	14.68(1)	14.14(2)	12.68(2)	12.33(1)
1,2,2	32.38(2)	28.40(2)	27.06(2)	–	–
1,2,1	25.27(1)	21.59(2)	19.37(3)	–	–
1,2,0	17.53(1)	14.05(2)	11.24(2)	8.89(2)	7.90(2)
1,3,0	–	–	13.7(1)	–	–
1,2,−1	–	–	–	−0.38(2)	–

[a] Cd^{2+}: 0.1 mol dm^{-3} KNO_3; all other metal ions: 0.1 mol dm^{-3} KCl. – [b] $\beta_{xyz} = [M_xL_yH_z] \times [M]^{-x} \times [L]^{-y} \times [H]^{-z}$; estimated standard deviations (in parentheses) were calculated with HYPERQUAD[36] and multiplied by a factor of three.

The results indicate that the two triamines *cis*-dap and *trans*-dap show a pronounced tendency to form protonated complexes of the compositions $[M(HL)]^{3+}$ and $[M(HL)_2]^{4+}$ in acidic solution (Figure 3). In the presence of excess ligand, the main species formed are the bis(complexes) $[ML_2H_x]^{(2+x)+}$. The formation of a tris(chelate) $[ML_3]^{2+}$ was only verified in the case of Ni^{II}. [Ni(*cis*-dap)$_3$]$^{2+}$ was seen as a minor species at the end of a titration using an excess of the ligand. In the experiments with total Ni/total *cis*-dap = 1:2, formation of [Ni(*cis*-dap)(H*cis*-dap)]$^{3+}$ and [Ni(*cis*-dap)]$^{2+}$ was observed in the same pH range, and a fixed value of β_{ML}, as obtained from an independent 1:1 titration, was used in the evaluation to avoid mutual influ-

Table 3. Formation constants for metal complexes with the diamine ligands (25 °C, 0.1 mol dm^{-3} KCl or KNO_3)

	Cu^{2+}			Ni^{2+}		Cd^{2+}[a]	
log β_{xyz}[b] x,y,z	ampy	*cis*-cptn	*trans*-cptn	ampy	*cis*-cptn	ampy	*cis*-cptn
1,1,0	8.24(1)	10.59(1)	8.58(1)	4.1(1)	7.02(1)	3.4(2)	5.20(1)
1,2,0	15.01(1)	19.75(1)	15.81(1)	8.1(1)	12.70(1)		9.52(1)
1,3,0					15.98(4)		
1,2,−1			8.97(3)			−2.1(1)	

[a] Cd^{2+}: 0.1 mol dm^{-3} KNO_3; all other metal ions: 0.1 mol dm^{-3} KCl. – [b] $\beta_{xyz} = [M_xL_yH_z] \times [M]^{-x} \times [L]^{-y} \times [H]^{-z}$; estimated standard deviations (in parentheses) were calculated with HYPERQUAD[36] and multiplied by a factor of three.

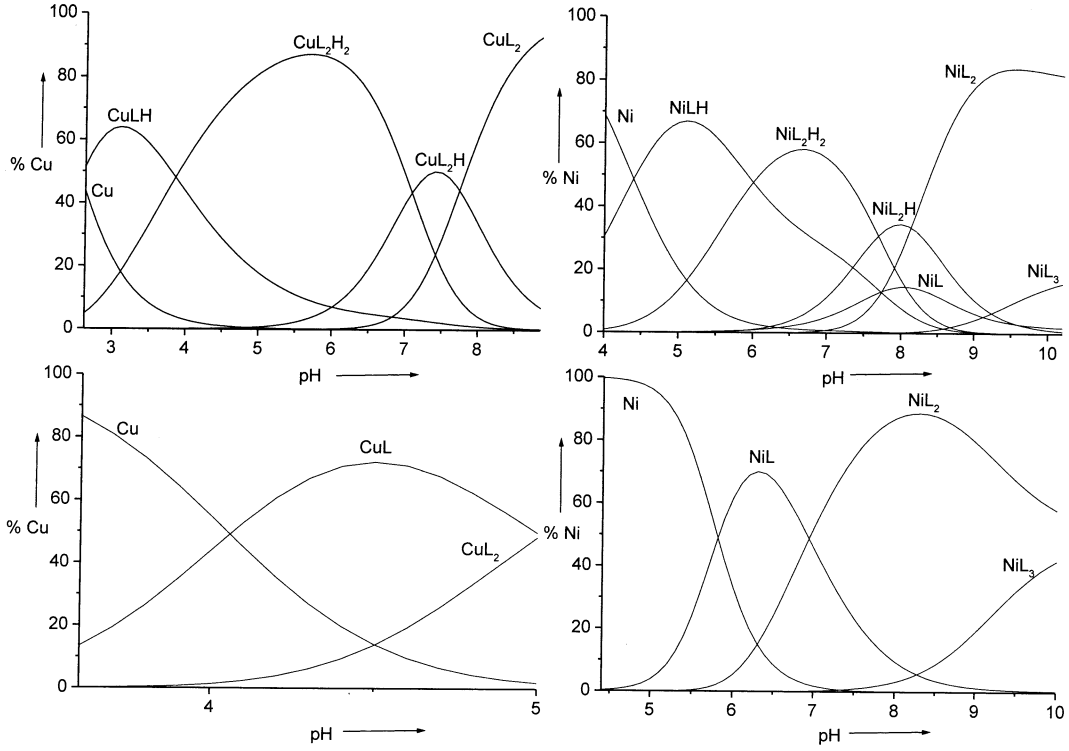

Figure 3. Species distribution plots for an equilibrated aqueous solution with a total metal ion (Ni, Cu) concentration of 10^{-3} mol dm^{-3} and a total ligand (L) concentration of 2×10^{-3} mol dm^{-3} (Cu) or 3×10^{-3} mol dm^{-3} (Ni); L = *cis*-dap (top), L = *cis*-cptn (bottom); only metal-containing species are shown; the equilibrium constants listed in Tables 2 and 3 were used for the calculations

ence (correlation effects) of the two formation constants. In the case of Cu^{II}, the unprotonated $[CuL]^{2+}$ complex was not observed.

As expected, the diamines ampy, *cis*-cptn, and *trans*-cptn do not form any protonated metal complexes and the titration curves could be evaluated simply in terms of $[ML]^{2+}$ and $[ML_2]^{2+}$ formation. In the case of *cis*-cptn and Ni^{II}, the formation of a complex of composition $[ML_3]^{2+}$ was additionally established. The complexation of Ni^{II} and Cd^{II} by ampy is rather weak and was only observed at pH > 8. To avoid precipitation of solid metal hydroxides, a large excess of ampy had to be used.

UV/Vis data of Ni^{II}- and Cu^{II}(amine) complexes provide a useful tool for assigning the structures of the different solution species.[14,15] The d-d transitions of Ni^{II} complexes with saturated amines are of rather low intensity ($\varepsilon \leq 10$) and hence rather concentrated solutions (0.1 M) had to be used. Under these conditions, both $[Ni(cis\text{-dap})_2]^{2+}$ and $[Ni(Hcis\text{-dap})_2]^{4+}$ form blue solutions, with $^3A_{2g}$-$^3T_{1g}(F)$ transitions at 571 and 577 nm, respectively. These values are consistent with an NiN_4O_2 chromophore and the minor shift upon deprotonation clearly indicates that incorporation of an additional nitrogen atom into the chromophore does not occur to any significant extent. We can therefore exclude both tridentate coordination and a bridging mode with the secondary nitrogen atom coordinated to an adjacent Ni^{II} center. In contrast to *cis*-dap, $[Ni(cis\text{-cptn})_2]^{2+}$ forms a bright-yellow solution (λ_{max} = 444 nm), indicative

of a diamagnetic complex.[10] It is noteworthy that the slightly less basic *cis*-dap does not form such a low-spin bis(complex). In the presence of excess *cis*-dap (Ni/L > 1:3), purple solutions with λ_{max} = 553 nm are observed. The considerable shift to shorter wavelengths is indicative of a tris(chelate) structure with an NiN_6 chromophore. Such an $[Ni(cis\text{-dap})_3]^{2+}$ complex had already been noted as a minor species in the aforementioned titration experiments. Since the significantly higher ligand concentration (0.3 mol dm^{-3}) favors complexation, the tris complex becomes the predominant species at pH > 10.

In aqueous solution, the d-d transitions of Cu^{II}(amine) complexes appear unresolved as a broad single band in the range 500−750 nm.[15] The intensity of this band is an order of magnitude higher than that seen for the corresponding Ni^{II} complexes, and this allowed the recording of solution spectra with a total Cu^{II} concentration of just 0.01−0.02 mol dm^{-3}. Measurements were made at an ionic strength of 1 mol dm^{-3} KNO_3 and were carried out in conjunction with an additional series of potentiometric titrations (Figure 4). These data allowed the determination of the stability constants by two independent methods. The agreement found was generally good (Table 4). Additionally, the measurements could be used for the calculation of spectra for each individual species (Figure 4, b). It is well established that for a tetragonally distorted geometry (C_{4v} or D_{4h}), successive replacement of the four water ligands by nitrogen donors in the equatorial plane results in a continuous shift of λ_{max} to shorter wavelengths, whereas substitution of the loosely bound axial water ligands results in a red shift (the "pentaammine effect").[16,17] $[Cu(H\textit{cis}\text{-dap})_2]^{4+}$, $[Cu(H\textit{cis}\text{-dap})(\textit{cis}\text{-dap})]^{3+}$, and $[Cu(\textit{cis}\text{-dap})_2]^{2+}$ were all found to exhibit absorbance maxima at 552−567 nm, indicative of a *trans*-CuN_4 chromophore. Similarly, the λ_{max} values of 560 nm (*trans*-dap), 550 nm (ampy), and 545 nm (*cis*-cptn)[18] indicate *trans*-CuN_4 geometries with one or two weakly bound water molecules at the apices in the corresponding bis complexes $[CuL_2]^{2+}$. The 1:1 complexes $[Cu(H\textit{cis}\text{-dap})]^{3+}$ (λ_{max} = 688 nm) and $[Cu(ampy)]^{2+}$ (λ_{max} = 668 nm) exhibit absorbance maxima at considerably longer wavelengths, as expected for *cis*-CuN_2 coordination.[14]

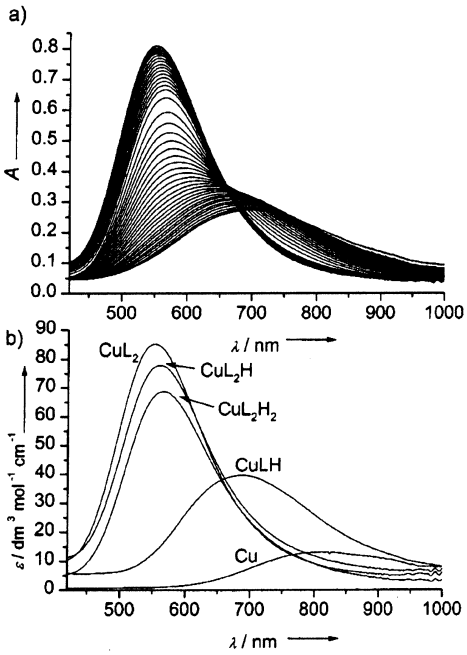

Figure 4. Spectral changes for the Cu^{II}(*cis*-dap) system during a titration experiment with total Cu = 10^{-2} mol dm^{-3} and total L = 2×10^{-2} mol dm^{-3} (a); the calculated spectra for the individual species (b)

Table 4. Comparison of formation constants of Cu^{II} complexes derived from either potentiometric (pot) or spectrophotometric (spec) titrations (25 °C, 1 mol dm^{-3} KNO_3) estimated standard deviations are given in parentheses

	pot[a]	spec[a]
log β_{xyz}[b]		
x,*y*,*z*		
ampy		
1,1,0	8.54(1)	8.53(1)
1,2,0	15.68(1)	15.65(2)
cis-dap		
1,1,1	17.64(2)	17.84(4)
1,2,0	18.41(2)	18.9(3)
1,2,1	26.62(2)	26.9(1)
1,2,2	34.23(2)	34.45(5)
trans-dap		
1,1,1	15.42(2)	15.63(3)
1,2,0	14.78(1)	14.9(2)
1,2,1	22.69(1)	22.93(9)
1,2,2	29.99(1)	30.27(5)

[a] Potentiometry: calculated with HYPERQUAD;[36] spectrophotometry: calculated with SPECFIT;[37] the obtained standard deviations are multiplied by a factor of three. − [b] $\beta_{xyz} = [M_xL_yH_z] \times [M]^{-x} \times [L]^{-y} \times [H]^{-z}$.

Structural Characterization of the Metal Complexes

In $[Pt(H\textit{cis}\text{-dap})Cl_4]Cl{\cdot}H_2O$, the ligand *cis*-dap coordinates to the Pt^{IV} center in a bidentate fashion through the two primary amino groups. The remaining secondary amino group of the pyrrolidine ring is protonated (Figure 5). The octahedral low-spin geometry of the Pt^{IV} center is completed by the coordination of four chloride ions. The positive charge of the complex cation is balanced by an additional chloride counterion. Considering the positions of the cations (A), represented by their centers of gravity, and of the counterions (B), the resulting AB-type packing can be described as a stack of layers consisting of fused six-membered rings with an alternating A−B−A−B−A−B sequence. The layers are oriented perpendicular to the *b* axis. This packing is related to the GeS structure,[19] although in GeS the six-membered Ge_3S_3 rings have a chair conformation, whereas in $[Pt(H\textit{cis}\text{-dap})Cl_4]Cl{\cdot}H_2O$ the A_3B_3 rings have a distorted boat conformation. In both cases, the nonisometric packing can be explained simply in terms of the nonisotropic shape of the cations. In $[Pt(H\textit{cis}\text{-dap})Cl_4]Cl{\cdot}H_2O$, the anions and cations within a layer are connected through N−H···Cl^- hydrogen bonds and the dif-

ferent layers are interconnected by N−H···O···H−N bridges between the coordinated amino groups and water molecules. The $[Pt(H\textit{cis}\text{-dap})Cl_4]^+$ complex cation is completely asymmetric as a consequence of the puckered conformation of the five-membered chelate ring. However, the NMR-spectroscopic data (two signals in the $^{13}C\{^1H\}$ NMR and three signals in the ^1H NMR spectrum) indicate the expected rapid ring inversion with average C_s symmetry for the complex in solution.

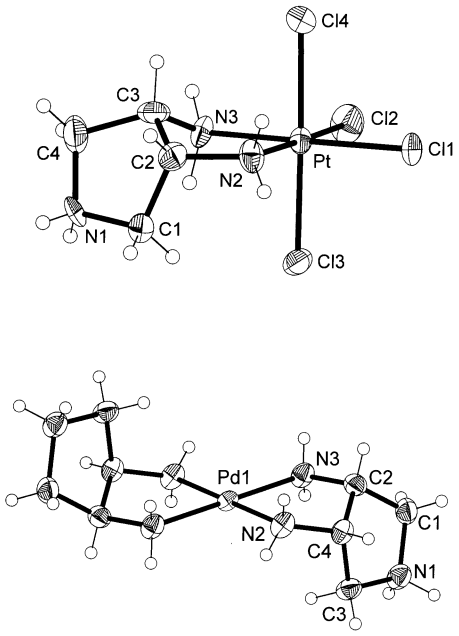

Figure 5. Molecular structures of $[Pt(H\textit{cis}\text{-dap})Cl_4]^+$ (top) and $[Pd(H\textit{cis}\text{-dap})_2]^{4+}$ (bottom); thermal ellipsoids are drawn at a 50% probability level; hydrogen atoms are shown as spheres of arbitrary size; selected bond lengths [Å] and angles [°]: (a) Pt−N2 2.075(10), Pt−N3 2.007(9), Pt−Cl1 2.333(3), Pt−Cl2 2.311(3), Pt−Cl3 2.322(3), Pt−Cl4 2.313(3), N2−Pt−N3 83.8(5); (b) Pd−N2 2.035(2), Pd−N3 2.039(2), N2−Pd−N3 83.86(9), N2−Pd−N3A 96.14(9)

A similar bidentate coordination of the protonated H*cis*-dap$^+$ ligand is observed for $[Pd(H\textit{cis}\text{-dap})_2](ClO_4)_4\cdot H_2O$ (Figure 5). The crystal structure of this compound can be described as a packing of neutral $\{[Pd(H\textit{cis}\text{-dap})_2](ClO_4)_4\}$ aggregates that are hydrogen-bonded through NH−H···OH−H···$OClO_3$···H−NH and NH−H···$OClO_3$···H−NH bridges. The Pd^{II} atom resides on a center of inversion and exhibits the well-known square-planar PdN_4 geometry (λδ conformation for the two five-membered chelate rings). The pyrrolidine rings are located at opposite sides of the PdN_4 plane and thus adopt a *transoid* orientation. A related structure with protonated endocyclic nitrogen atoms in a *transoid* geometry has been reported by Schwarzenbach et al. for the Pd complex of *cis*-3,5-diaminopiperidine (dapi).[4] These authors performed a potentiometric study to determine the acidity constants of the noncoordinating ammonium groups of $[Pd(Hdapi)_2]^{4+}$; an unusually slow equilibration was noted, which was discussed in terms of a slow rearrangement of the ligands (a change from the *transoid* to the *cisoid* form in the course of deprotonation). The required breaking and reforming of Pd^{II}−N bonds was invoked to account for the slow reaction rate. In our experiments, we found a related steady shift of pH for a freshly prepared 0.1 mol dm^{-3} aqueous solution of $[Pd(H\textit{cis}\text{-dap})_2](ClO_4)_4$. However, this shift proved to be very slow (5 mV per 24 h) and the data set of a rapid titration could be evaluated in terms of a simple two-step deprotonation with pK_a values of 6.27(1) and 7.04(1).

With Cu^{II}, a solid sample of composition $[Cu(H\textit{cis}\text{-dap})_2(OH_2)_2](SO_4)_2\cdot 3.5H_2O$ was obtained. This compound contains two crystallographically independent $[Cu(H\textit{cis}\text{-dap})_2(OH_2)_2]^{4+}$ cations (Figure 6). Cu1 is located on a twofold axis and its five-membered chelate rings thus have a λλ or δδ conformation, whereas Cu2 resides on a center of inversion with a λδ conformation of the rings. Again, the Cu centers are exclusively bound to the primary amino groups of the H*cis*-dap$^+$ ligands (square-planar $Cu^{II}N_4$ geometry with an average Cu−N bond length of 2.02 Å). The coordination sphere is completed by two loosely bound water ligands in the axial positions (average Cu−O bond length: 2.48 Å), giving the well-known tetragonally distorted CuN_4O_2 octahedron. The noncoordinating ring nitrogen atoms are protonated and the pyrrolidine rings are arranged in a *transoid* manner, akin to that described above for the Pd complex. Deprotonation of $[Cu(H\textit{cis}\text{-dap})_2(OH_2)_2]^{4+}$ could occur either at the noncoordinating ring nitrogen atoms or at the water ligands (with the formation of hydroxo complexes). In the first case, the liberation of an additional amino group would generate a potentially tridentate ligand. The additional amino group could either coordinate in a tripodal intramolecular fashion or intermolecularly as a bridging ligand to an adjacent metal center. The crystal structure of $[Cu(H\textit{cis}\text{-dap})_2(OH_2)_2](SO_4)_2\cdot 3.5H_2O$ provided evidence that the latter mode is observed with Cu^{II}. Close inspection of the difference Fourier map revealed a residual peak at $x = 3/4$, $y = 1/4$, $z = 0.2736$ with an electron density of 1.6 e/Å^3. This peak is located on a twofold axis in a cavity formed by the noncoordinating ammonium groups of two complex cations, two sulfate counterions, and a water molecule. The distances to the nearest atoms are 2 × 1.96 Å (O22 & O22A), 2.00 Å (O60), 2 × 2.19 Å (N1 & N1A). Further studies of additional specimens showed considerable variation in the intensity of this peak. Although the cell parameters and atom positions were almost the same for all the samples under investigation, the intensity of this peak corresponded to an electron density of up to 12.6 eÅ^{-3}. Based on the chemical composition of the mother liquor, the charge balance, and the distances to the five nearest neighboring atoms, we interpret this peak in terms of some additional incorporation of Cu^{II}, which is bound to the two pyrrolidine nitrogen atoms with the abstraction of two protons (Scheme 3). In fact, it became clear that this compound has a nonstoichiometric (berthollide) composition, for which the correct formula would be $[Cu(H\textit{cis}\text{-dap})_2(OH_2)_2](SO_4)_2\cdot 3.5\ H_2O - 2x\ H^+ + x\ Cu^{2+}$. In this study, the data for $x = 0.005$, 0.08, and 0.11 are reported. Although the cavity appears to

have an almost ideal size for accommodating Cu^{II}, some minor structural rearrangements are evidently required for the uptake of an additional Cu^{II} ion. This is indicated by a disorder that is found for those samples containing a large amount of additional Cu. This disorder is manifested in strong anisotropy of the displacement parameters for the atoms of the outer part of the pyrrolidine rings and the observation of two partially occupied positions for one of the oxygen atoms of the sulfate residue (Figure 6). The additional Cu^{II} center has trigonal-bipyramidal coordination with the two pyrrolidine nitrogen atoms in the axial positions and two sulfate ions and a water molecule in the equatorial positions. This additional Cu^{II} center interconnects two mononuclear $[Cu(H\textit{cis}\text{-dap})_2(OH_2)_2]^{4+}$ cations giving a trinuclear $[(H\textit{cis}\text{-dap})Cu(OH_2)_2(\mu\text{-}\textit{cis}\text{-dap})Cu(OH_2)(SO_4)_2(\mu\text{-}\textit{cis}\text{-dap})Cu(H\textit{cis}\text{-dap})(OH_2)_2]^{4+}$ entity. The observation of such trinuclear species nicely illustrates the ability of the neutral *cis*-dap molecule to participate in bridging interactions, and we regard this ligand as an interesting building block for the construction of coordination polymers.

A complex featuring a tridentate coordination mode of *cis*-dap, with all the nitrogen atoms of the ligand bound to the same metal center, could be obtained in the form of the heteroleptic $[Co^{III}(\textit{cis}\text{-dap})(tach)]^{3+}$. Attempts to prepare a homoleptic complex $[Co(\textit{cis}\text{-dap})_2]^{3+}$ by aerial oxidation of a solution of Co^{II} and *cis*-dap failed and the use of Co^{III} precursors such as $K_3[Co(CO_3)_3]$ or *trans*-$[CoCl_2(py)_4]Cl$ led to unresolved reaction mixtures. $[Co(\textit{cis}\text{-dap})(tach)]^{3+}$ was prepared from $[Co(tach)Cl_3]$, in which the relatively labile Cl^- ligands define a set of leaving groups having the required preformed facial geometry. The resulting mononuclear Co^{III} complex was crystallized as a chloride tetrachlorozincate salt. Its hexaamine geometry exhibits some rather unusual features. Bond lengths and angles for the Co(tach) moiety all fall within the expected ranges (Figure 7), whereas the $Co^{III}-N$ bonds in the Co(*cis*-dap) moiety are remarkably long. This is particularly true for the secondary nitrogen atom, which has a Co−N distance of 2.068(5) Å. The puckering parameters [$Q = 0.601(4)$ Å and $\varphi = 0.8(4)°$] for the pyrrolidine ring correspond to an almost ideal envelope conformation. This conformation implies an eclipsed orientation of the two CH protons with a torsional angle of only 8.7°, a rather short (N−)H···H(−N) separation of 2.24 Å for the primary amino groups, and a significantly elongated C7−C8 bond (1.60 Å). Owing to the rather long

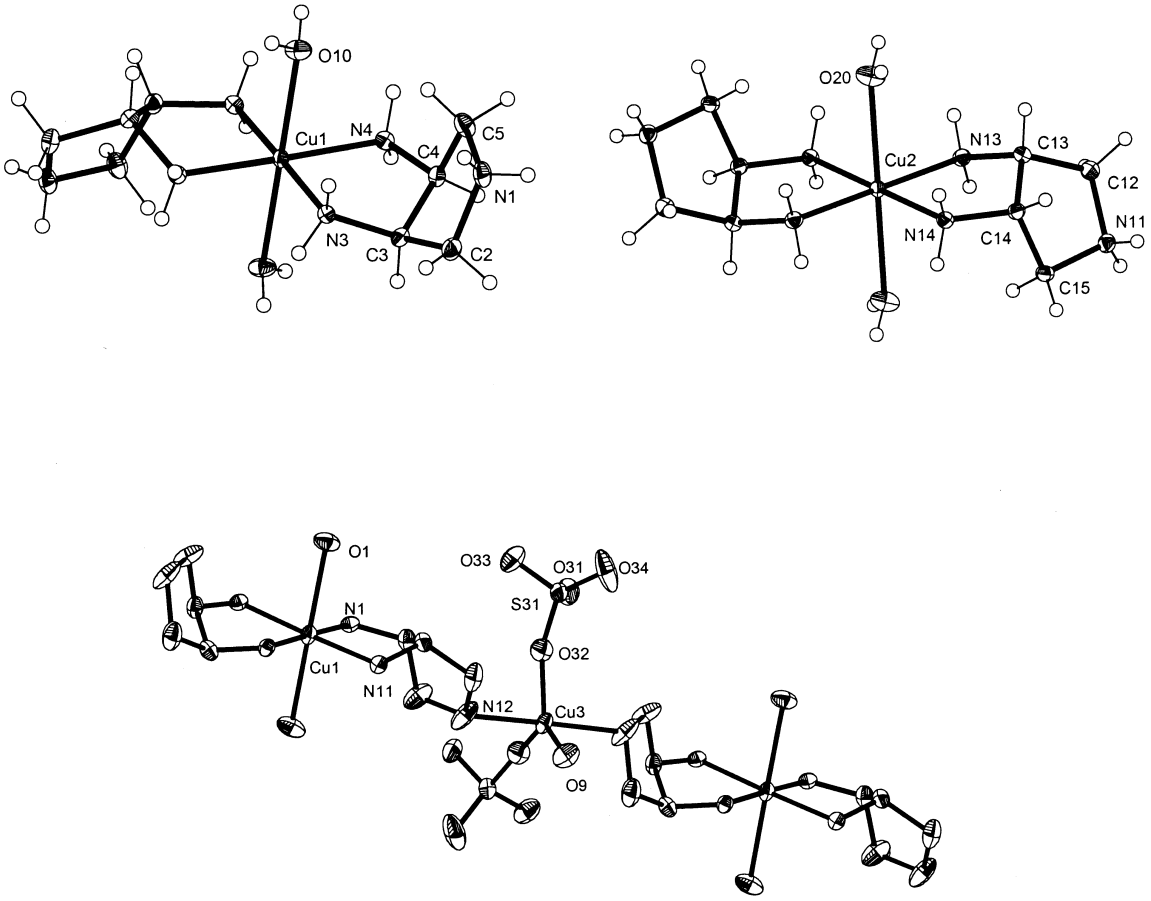

Figure 6. Structural representations of $[Cu(H\textit{cis}\text{-dap})_2(OH_2)_2](SO_4)_2{\cdot}3.5H_2O - 2x\ H^+ + x\ Cu^{2+}$: the two $[Cu(H\textit{cis}\text{-dap})_2(OH_2)_2]^{4+}$ cations for $x < 0.01$ (top); hydrogen atoms are shown as spheres of arbitrary size; selected bond lengths [Å] and angles [°]: Cu1−N3 2.0174(13), Cu1−N4 2.0271(13), Cu1−O10 2.4660(12), Cu2−N13 2.0144(13), Cu2−N14 2.0186(13), Cu2−O20 2.4985(13), N3−Cu1−N4 84.40(5), N13−Cu2−N14 84.73(5); view of the trimer with the partially occupied Cu3 position ($x = 0.11$) (bottom); hydrogen atoms are omitted for clarity; in the absence of Cu3 the ring nitrogen atom N12 is protonated, forming a hydrogen bond to the SO_4^{2-} counterion (O32); only one of the two positions of the disordered O32 is shown; thermal ellipsoids are drawn at a 50% probability level

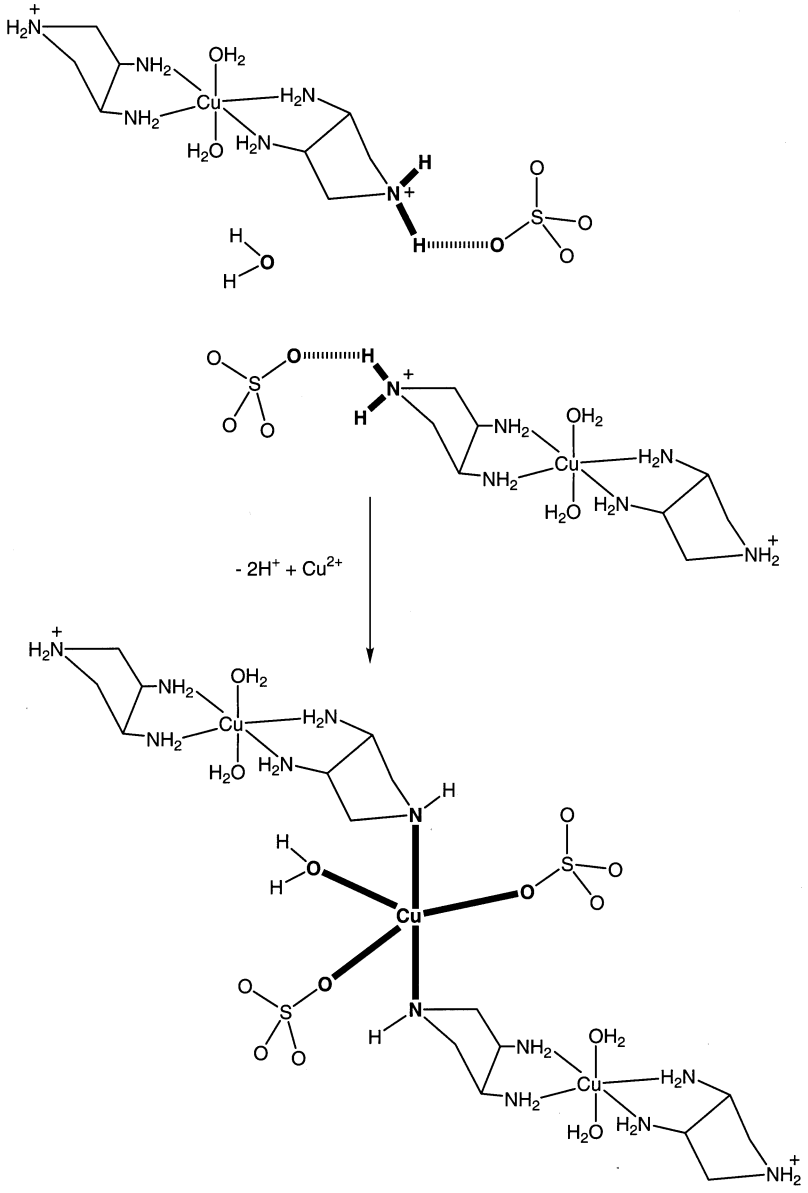

Scheme 3

$Co^{III}-N$ bonds in the Co(*cis*-dap) moiety, a decrease in ligand field and an increased tendency to form the corresponding Co^{II} complex could be expected.[20] However, [Co(*cis*-dap)(tach)]$^{3+}$ exhibits the usual yellow color with absorbance maxima at 351 and 475 nm, as expected for a normal Co^{III}(hexaamine) chromophore.[21] Cyclic voltammetry revealed quasi-reversible redox behavior with a redox potential of −0.21 V (versus NHE). Compared to the range usually observed for Co^{III}(hexaamine) complexes (0.3−0.5 V versus NHE), the potential of [Co(*cis*-dap)(tach)]$^{2/3+}$ indicates only a minor degree of stabilization of the Co^{II} species.[5,20,21]

The diamine ligands *cis*-cyclopentane-1,2-diamine (*cis*-cptn) and 3-aminopyrrolidine (ampy) have been included in this investigation as structural models for a coordination of a metal cation to either two exocyclic nitrogen donors or to one exocyclic and one endocyclic nitrogen donor, respectively. Toftlund et al. have previously reported the preparation of the yellow, diamagnetic complex [Ni(*cis*-cptn)$_2$]$^{2+}$.[10] We have crystallized this species as [Ni(*cis*-cptn)$_2$](ClO$_4$)$_2$ and report its crystal structure (Figure 8). As expected for a diamagnetic complex, the Ni center has a square-planar NiN_4 geometry with an average Ni−N bond length of 1.92 Å. Again, the two cyclopentane rings have a *transoid* arrangement with respect to the NiN_4 plane. [Cu(ampy)$_2$]$^{2+}$, which has also been crystallized as its perchlorate salt (Figure 8), represents an example of a structure where both endo- and exocyclic nitrogen donors are used for metal binding.[22−24] The ligand was used as a racemate and the crystal structure of [Cu(3*R*-ampy)(3*S*-ampy)](ClO$_4$)$_2$ showed the incorporation of both enantiomers in one complex entity. The Cu^{II} center has square-planar

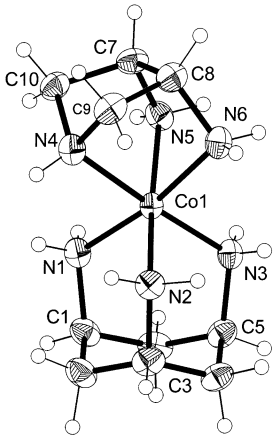

Figure 7. Molecular structure of $[Co(cis\text{-dap})(tach)]^{3+}$; thermal ellipsoids are drawn at a 50% probability level; hydrogen atoms are shown as spheres of arbitrary size; selected bond lengths [A] and angles [°]: Co−N2 1.958(6), Co−N3 1.964(5), Co−N1 1.966(4), Co−N6 1.975(4), Co−N5 2.001(7), Co−N4 2.068(5), C7−C8 1.598(5); the other C−C bonds range from 1.518(6) to 1.532(5); N6−Co−N5 76.27(15), N5−Co1−N4 85.2(3), N6−Co1−N4 84.4(2); intraligand N−Co−N angles in the Co(tach) moiety range from 89.4(3) to 92.40(14)

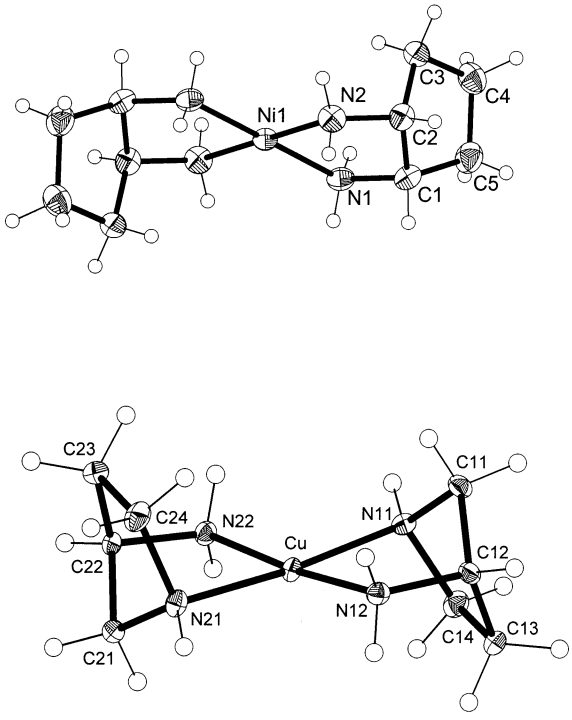

Figure 8. Molecular structures of $[Ni(cis\text{-cptn})_2]^{2+}$ (top) and $[Cu(3R\text{-ampy})(3S\text{-ampy})]^{2+}$ (bottom); thermal ellipsoids are drawn at a 30% probability level; hydrogen atoms are shown as spheres of arbitrary size; selected bond lengths [A] and angles [°]: Ni−N1 1.928(3), Ni−N2 1.916(3), N2−Ni−N1 86.01(14); Cu−N11 2.027(4), Cu−N12 2.013(4), Cu−N21 2.027(4), Cu−N22 2.010(4), N22−Cu−N12 174.4(2), N12−Cu−N11 95.91(17), N21−Cu−N11 174.8(3), N22−Cu−N11 95.91(17), N12−Cu−N21 98.18(16), N22−Cu−N21 82.44(17)

CuN_4 geometry with a very weak interaction with one of the ClO_4^- counterions. The two endocyclic and the two exocyclic nitrogen donors each have a *trans* orientation. Each Cu(ampy) fragment can be regarded as a metalla derivative of norbornane. By analogy with the structure of this hydrocarbon,[25] the geometry at the bridging methylene groups deviates significantly from a tetrahedral arrangement (N−C−C angles: 98.9° and 97.6°) and, compared to the corresponding *cis*-cptn system, the M(ampy) structure appears to be considerably strained.

Discussion

Equilibria in Aqueous Solution

A comparison of the protonation constants of *cis*-dap, *trans*-dap, *cis*-cptn, *trans*-cptn, ampy, and related amines (Table 5) indicates some characteristic trends. Compared to related monoamines such as cyclopentylamine ($pK_a = 10.6$) or pyrrolidine ($pK_a = 11.2$),[26] the triamines *cis*-dap and *trans*-dap are weaker bases. On statistical grounds, the presence of three basic sites should increase the overall basicity; however, it seems that the electron-withdrawing influence of additional amino groups outweighs this effect. In contrast to the monoamine analogues, the ^1H NMR titration did not show a significant difference for the intrinsic basicities of the primary and secondary amino groups in *cis*-dap[5] and it appears that the different behavior of the individual diastereomers is based on steric rather than electronic effects. The cyclopentane or pyrrolidine frameworks give rise to particularly rigid molecules and the different basicities of the diastereomers can simply be explained in terms of electrostatic repulsion. In H_2*trans*-$cptn^{2+}$, the two amonio groups adopt a staggered (antiperiplanar) conformation and the relevant pK_a values of H_2*trans*-$cptn^{2+}$ are in close agreement with those of the open-chained H_2en^{2+} (en = ethane-1,2-diamine): the difference $pK_1 - pK_2 = \Delta pK$ is 2.70 for H_2*trans*-$cptn^{2+}$ and 2.80 for H_2en^{2+}. In H_2*cis*-$cptn^{2+}$, the interatomic distance between the two positive charges is shorter and consequently ΔpK_a for this isomer is increased to 3.60. Analogously, the acidity constants of monoprotonated H*cis*-dap^+ and H*trans*-dap^+ are in close agreement, whereas those of the triply protonated forms differ considerably with the *cis* isomer being the stronger acid.

Analysis of the formation constants together with the spectroscopic properties of *cis*-dap complexes in aqueous solution points to a bidentate rather than a tridentate coordination mode for this ligand:

(i) Ni^{II} forms a tris(chelate) with an NiN_6 chromophore, whereas the λ_{max} values of the two bis(complexes) $[Ni(cis\text{-dap})_2]^{2+}$ and $[Ni(Hcis\text{-dap})_2]^{4+}$ are both indicative of an NiN_4 chromophore.[14] Clearly, deprotonation of the ammonium groups is not followed by metal binding, and a third ligand is required to achieve hexaamine formation. Similarly, the bis(complexes) $[CuH_xL_2]^{(2+x)+}$ ($0 \le x \le 2$, L = *cis*-dap, *trans*-dap; and $x = 0$, L = *cis*-cptn) all show a characteristic band in their visible spectra with an absorption maximum at 550−570 nm (Table 6). These values are

Table 5. Comparison of protonation (log K_i) and complex formation constants (log β_2) for some selected polyamines

Polyamine[a]	log K_3[b]	H^+ log K_2	log K_1	Cu^{II} log β_2[c]	Ni^{II} logβ_2
Triamines					
cis-dap	2.4	6.3	9.7	17.5	11.2
trans-dap[d]	3.7	6.3	9.6	14.1	–
trap	3.6	7.9	9.6	19.6	17.4
tmca	5.2	6.9	9.3	23.6	25.9
dapi	4.2	7.6	9.5	20.1	21.2
Diamines					
cis-cptn		6.1	9.7	19.8	12.7
trans-cptn[e]		7.2	9.9	15.8	–
cis-chxn		6.3	9.7	20.0	13.8
trans-chxn[e]		6.6	9.8	21.1	14.3
ampy[e]		6.8	10.4	15.0	8.1
en		7.1	9.9	19.6	13.4

[a] Abbreviation of ligands and references: *cis*-dap = *cis*-3,4-diaminopyrrolidine; *trans*-dap = *trans*-diaminopyrrolidine; trap = 1,2,3-propanetriamine;[27] tmca = all-*cis*-2,4,6-trimethoxycyclohexane-1,3,5-triamine;[28] dapi = *cis*-3,5-piperidinediamine;[5] *cis*-cptn = *cis*-cyclopentane-1,2-diamine; *trans*-cptn = *trans*-cyclopentane-1,2-diamine; *cis*-chxn = *cis*-cyclohexane-1,2-diamine;[26] *trans*-chxn = *trans*-cyclohexane-1,2-diamine;[26] ampy = 3-aminopyrrolidine; en = ethane-1,2-diamine[26]. – [b] $K_i = [H_iL] \times [H]^{-1} \times [H_{i-1}L]^{-1}$. – [c] $\beta_2 = [ML_2] \times [M]^{-1} \times [L]^{-2}$. – [d] (3*R*,4*R*) enantiomer. – [e] Racemate.

Table 6. UV/Vis data for Ni^{II}- [$^3A_{2g}$-$^3T_{1g}(F)$ transition] and Cu^{II}-(amine) complexes in aqueous solution (25 °C)

Complex	λ_{max} [nm]	ε
$[Cu(Hcis\text{-dap})]^{3+}$	688	40
$[Cu(cis\text{-dap})_2]^{2+}$	552	86
$[Cu(cis\text{-dap})(Hcis\text{-dap})]^{3+}$	566	69
$[Cu(Hcis\text{-dap})_2]^{4+}$	561	78
$[Cu(trans\text{-dap})_2]^{2+}$	560	140
$[Cu(ampy)]^{2+}$	668	64
$[Cu(ampy)_2]^{2+}$	550	142
$[Cu(cptn)_2]^{2+}$	545	92
$[Ni(cis\text{-dap})_2]^{2+}$	571	8
$[Ni(Hcis\text{-dap})_2]^{4+}$	577	6
$[Ni(cis\text{-dap})_3]^{2+}$	553	10

indicative of a *trans* (square-planar) CuN_4 chromophore with additional loosely bound water molecules at the apices.[14] It is well known that the coordination of an additional *nitrogen* donor in an apical position would lead to a significant red shift (pentaammine effect).[16] The close similarity of the spectral properties of the differently protonated species again indicates that deprotonation at the third nitrogen atom does not result in a significant rearrangement of the chromophore.

(ii) Compared to other tridentate cyclic triamines such as 3,5-diaminopiperidine (dapi) or all-*cis*-2,4,6-trimethoxycyclohexane-1,3,5-triamine (tmca), the formation constants for $[M(cis\text{-dap})_2]^{2+}$ are remarkably low (Table 5). The formation constants of $[M(cis\text{-dap})]^{2+}$ are about one order of magnitude lower than those of $[M(en)]^{2+}$. For the 1:2 complexes, this effect is doubled.

(iii) As a consequence of the Jahn–Teller distortion, triamine ligands that are restricted to a tripodal, facial coordination usually show a characteristic inversion of the Irving–Williams series with higher stability for Ni^{II} than for Cu^{II}. For *cis*-dap, however, no such inversion is observed. As shown in Figure 9, the stabilities of the *cis*-dap complexes fall in the expected range based on the linear free-energy relationship of log β_{Ni} vs. log β_{Cu} for "normal" open-chained polyamines.

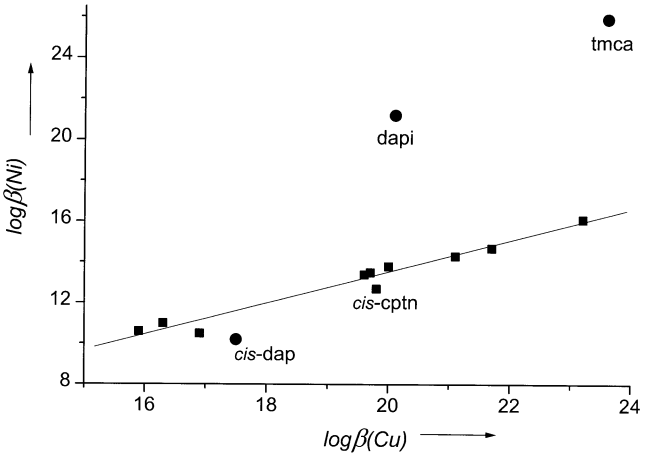

Figure 9. Comparison of formation constants for Cu^{II}- and Ni^{II}(amine) complexes; the linear free-energy relationship (squares) for selected diamines (log β_2), triamines $H_2N-(CH_2)_x-NH-(CH_2)_y-NH_2$ (log β_1), and tetraamines $H_2N-(CH_2)_x-NH-(CH_2)_y-NH-(CH_2)_z-NH_2$ (log β_1) is $\log \beta_{Ni} = 0.77 \times \log \beta_{Cu} - 1.84$; this is compared with log β_2 values of the potentially tripodal ligands *cis*-dap, dapi, and tmca (circles); the data are from refs.[5,25,27] and from this work (Tables 2 and 3)

(iv) All the *cis*-dap complexes show a pronounced tendency to form protonated species $[M^z(HL)]^{(z+1)+}$, $[M^z(HL)_2]^{(z+2)+}$, and $[M^z(HL)L]^{(z+1)+}$. $[Pt(Hcis\text{-dap})Cl_4]^+$, $[Pd(Hcis\text{-dap})_2]^{4+}$, and $[Cu(Hcis\text{-dap})_2(OH_2)_2]^{4+}$ are representative examples that have been structurally characterized by single-crystal X-ray diffraction analysis. For the divalent metal cations (M = Ni, Cu, Zn, Cd), the pK_a values for deprotonation of the partially protonated complexes fall in the range 7.1–8.1, indicating only a slight decrease in the basicity of *cis*-dap upon coordination. This effect would be incompatible with a significant interaction between the third amino group and the metal cation. It is also noteworthy that the pK_a values of $[Cu(HL)_2]^{4+}$ are very similar for L = *cis*-dap and L = *trans*-dap (7.1, 7.7 versus 6.8, 7.5, respectively). The *trans* isomer is even slightly more acidic. Since tridentate coordination of *trans*-dap can be ruled out on steric grounds, the even higher basicity of $[Cu(cis\text{-dap})_2]^{2+}$ would again be inconsistent with a significant interaction between the third nitrogen atom and the metal cation.

The arguments listed as (i)–(iv) clearly show that tridentate coordination of *cis*-dap is not observed in labile solution species. Additionally, monodentate coordination of any of

the studied ligands can also be excluded. Although some of the bis(complexes), particularly $[M(ampy)_2]^{2+}$ (M = Ni, Cu, Cd) and $[Cu(trans\text{-}dap)_2]^{2+}$, show rather low stabilities, their formation constants are still considerably higher than those for monodentate amines such as NH_3 or CH_3NH_2. Moreover, not only *cis*-dap but all the other ligands as well give rise to a visible spectrum for $[CuL_2]^{2+}$ that is indicative of a *trans*-CuN_4 chromophore.

The solid-state structures of $[Pt(Hcis\text{-}dap)Cl_4]^+$, $[Pd(Hcis\text{-}dap)_2]^{4+}$, and $[Cu(Hcis\text{-}dap)_2(OH_2)_2]^{4+}$ reveal exclusive coordination of the metal cation to the two primary amino groups. Although the potentiometric measurements do not of course allow a direct structural assignment, comparison of *cis*-dap with the model diamines provided ample evidence for a similar binding to the exocyclic nitrogen atoms in solution: Metal complexes of ampy are generally less stable than the corresponding *cis*-cptn complexes. Clearly, coordination to the two exocyclic donors is preferred. Molecular mechanics calculations on $[Cu(cis\text{-}dap)(OH_2)_4]^{2+}$ also showed that coordination to the two primary amino groups would be favored by about 9.3 kJ mol^{-1}. For $[Cu(cis\text{-}cptn)]^{2+}$ and $[Cu(ampy)]^{2+}$ the difference in stability ($\Delta\log\beta_1$) is 2.4, corresponding to a difference in free enthalpy of 13.5 kJ mol^{-1}.

Comparison of the metal complex stabilities of the different ligands investigated in this study reveals the order *cis*-cptn > *cis*-dap > *trans*-cptn > ampy > *trans*-dap. Regarding $[Cu(HL)]^{3+}$ formation, the formation constant of the *trans*-dap complex is lowered by about two orders of magnitude compared with that of the *cis*-dap derivative, and for the bis(complexes) $[Cu(HL)_2]^{4+}$, $[Cu(HL)L]^{3+}$, and $[CuL_2]^{2+}$ the decrease in stability is about four orders of magnitude. Similar effects are observed for *trans*-cptn and *cis*-cptn. The *cis*-cyclopentane-1,2-diamine structure is clearly favorable with regard to metal binding. This is in contrast to the cyclohexane-1,2-diamine structure, for which the *trans* isomer has been reported to be more stable.[26] The formation constants of the *cis*-cptn complexes are in close agreement with those reported for the corresponding en complexes. Evidently, the *cis*-cyclopentane-1,2-diamine framework does not provide any stabilization in terms of pre-organization of the donor groups. Again, this is in contrast to the cyclohexanediamines, where significantly increased stability is observed for the *trans*-cyclohexane-1,2-diamine. Since *cis*-cptn and *cis*-dap have related structures, the reduced ability of the latter to bind metal cations must be interpreted in terms of a lower nucleophilicity of the donor groups, caused by the electron-withdrawing effect of the endocyclic nitrogen atom. Consequently, the higher ligand field of *cis*-cptn is able to generate a low-spin electron configuration for $[Ni(cis\text{-}cptn)_2]^{2+}$, whereas $[Ni(cis\text{-}dap)_2]^{2+}$ is high spin. Similar considerations are applicable for the *trans*-cptn and *trans*-dap systems. The observed decrease in metal complex stability in the above series can thus be rationalized in terms of a combination of steric (a) and electronic (b) effects:

(a) For the five-membered ring frame, a steady decrease in metal complex stability is observed for the following geometries: two exocyclic nitrogen atoms in a *cis* arrangement > two exocyclic nitrogen atoms in a *trans* arrangement > one endocyclic and one exocyclic nitrogen atom.

(b) Since all the ligands coordinate in a bidentate fashion, the presence of an additional nitrogen atom reduces the nucleophilicity of the donor groups and, consequently, the triamines are generally weaker ligands than the corresponding diamines.

Although in terms of absolute stability, the metal binding ability of the triamines is lower, the opposite behavior is observed in neutral and acidic solutions. This is based upon the ability of the dap complexes to bind additional protons, which is, of course, not possible for the diamines. In terms of conditional stability,[29] *cis*-dap is a rather efficient complexing agent for Cu^{II} in acidic solution and is clearly superior to any of the known aliphatic or alicyclic diamines. It is in fact a remarkable property of this ligand that it is capable of significant complexation even under acidic conditions, such as at pH = 2.5 (Figure 3).

Structural Aspects of the Metal Complexes

Although the coordination behavior of *cis*-dap in labile complexes must be regarded as being mainly bidentate, in principal a facial tridentate coordination is possible, as exemplified by the inert Co^{III} complex $[Co(cis\text{-}dap)(tach)]^{3+}$. However, the structural parameters for this complex, particularly the long Co−N bonds, clearly reveal a severely strained structure. We were unable to model this particular $Co^{III}N_6$ geometry with a commercially available MM program.[30,31] It seems that a nonharmonic description of the Co^{III}−N bond would be required, which was not implemented by the force field used. In a complex with bidentate coordination, the noncoordinating endocyclic nitrogen atom can either accept a proton or bind to an additional metal center. The first possibility has been discussed extensively for solid-state and solution species in the previous section. Although we do not have any experimental evidence that the latter possibility is realized in aqueous solution, the crystal structure of $[Cu(Hcis\text{-}dap)_2(OH_2)_2](SO_4)_2{\cdot}3.5H_2O - 2x\ H^+ + x\ Cu^{2+}$, with its nonstoichiometric composition ($0.01 \le x \le 0.11$) shows that multiple binding of metal cations to a *cis*-dap molecule is at least possible in the solid state. It is noteworthy that *cis*-dap is structurally related to the open-chained propane-1,2,3-triamine (trap): The trap molecule can be regarded as a substructure of *cis*-dap. However, the open-chained trap is conformationally flexible whereas *cis*-dap is rigid, thus representing a model of the triamine with a locked conformation. Interestingly, the coordination behavior of these two ligands towards Cu^{II} is similar. The ligand trap, by analogy with *cis*-dap, forms similar protonated Cu complexes in acidic solution, and a bridging mode with bidentate and monodentate coordination has been established from the crystal structure of $[Cu(trap)_2]Cl_2$.[27] However, it appears that the locked conformation is not optimal for metal binding: The trap complexes are generally more stable than the corresponding *cis*-dap analogues. Moreover, with other metal cations such as Ni^{II}, the flexibility of trap allows tridentate coordination, which

is not accessible for *cis*-dap. Analogously, the structure of *trans*-dap represents another conformation of trap that is even more disfavored for metal binding.

Another interesting aspect is the comparison of the three cyclic triamine ligands tach, dapi, and *cis*-dap (Scheme 1). The ligand tach shows a very pronounced preference for facial tridentate coordination, giving an adamantane-like structure with all six-membered chelate rings. Attempts to enforce a bidentate coordination mode failed. Reaction with Pt^{II} resulted in oxidation to Pt^{IV} with a concomitant facial coordination of tach.[32] On the other hand, *cis*-dap shows a strong preference for bidentate coordination. A facial, tridentate coordination mode comprising exclusively five-membered chelate rings is severely strained. Such an [M(*cis*-dap)] structure can formally be derived from the [M(tach)] moiety by the removal of one CH_2 and one CH group. The [M(dapi)] structure contains one six-membered and two five-membered chelate rings, in analogy to noradamantane. As a true intermediate in this series, dapi predominantly coordinates in a tridentate mode. However, bidentate coordination is possible, as has been observed for Pd^{II}.[4]

Conclusion

The basic coordination mode of the cyclic triamine *cis*-3,4-diaminopyrrolidine is a bidentate coordination through the two exocyclic amino groups. This mode has been established in a variety of solid-state structures. The potentiometric data and the spectroscopic properties of *cis*-dap complexes have also provided evidence for this coordination mode in aqueous solution. The noncoordinated endocyclic nitrogen atom represents a comparatively strong basic site, and as such it is readily protonated. A facial, tridentate coordination mode results in a highly strained structure, as shown for the inert $[Co(\textit{cis}\text{-dap})(tach)]^{3+}$. The formation of such strained species is not trivial and requires specific synthetic strategies. Alternatively, coordination of *cis*-dap to two different metal cations is possible. In this mode, one metal cation is bound through the primary amino groups, whereas the other is coordinated to the endocyclic nitrogen donor. The coordination behavior of *cis*-dap is in marked contrast to that of other cyclic triamine ligands such as *cis*-3,5-diaminopiperidine or all-*cis*-cyclohexane-1,3,5-triamine, where bidentate coordination or a bridging mode are of minor importance or even unknown.

Experimental Section

Safety Notes: Organic polyazides and perchlorate salts of metal complexes with organic ligands are potentially explosive. The organic polyazides should only be handled in dilute solutions and should not be isolated as pure substances. The perchlorate salts should only be isolated in small quantities and should not be dried at elevated temperatures.

Instrumentation: ^1H and $^{13}C\{^1H\}$ NMR spectra were measured in D_2O, $CDCl_3$, CD_3CN, or [D_6]acetone at 28 °C with a Bruker DRX 500 MHz NMR spectrometer (resonance frequencies: 500.13 MHz for ^1H and 125.9 MHz for $^{13}C\{^1H\}$). Chemical shifts are given relative to [D_4]sodium (trimethylsilyl)propionate (D_2O) or tetramethylsilane (all other solvents) as internal standards ($\delta = 0$). pD values (corrected)[5] were determined with a glass electrode. The ^1H NMR titration experiment on *cis*-dap was performed and evaluated as reported previously for dapi.[5] – UV/Vis spectra of the Ni^{II} complexes were measured with a Uvikon 941 spectrophotometer (H_2O; 25 ± 3 °C). – Cyclic voltammograms were recorded as described previously (BAS C2 cell, BAS 100B/W2 potentiostat, Au working electrode, Pt counter electrode, Ag/AgCl reference electrode, ambient temperature).[5] – C,H,N analyses were performed by H. Feuerhake (Universität des Saarlandes).

Materials: Unless otherwise stated, all chemicals used for the synthetic work were commercially available products of reagent-grade quality. For the potentiometric and spectrophotometric titrations, metal salts of highest available quality (> 99.95%) were used. 3-Pyrroline[33] and (3*S*,4*S*)-1-benzyl-3,4-pyrrolidinediyl bis(methanesulfonate)[34] were prepared as described in the literature. [Co(tach)$(NO_3)_3$] was obtained from [Co(tach)Cl_3].[35] Dowex 50 W-X2 (100–200 mesh, H^+ form) and Dowex 2-X8 (50–100 mesh, Cl^- form) were purchased from Fluka. The anion resin was converted into the OH^- form using dilute aqueous NaOH.[5]

1-Acetyl-3-pyrroline: To an ice-cooled solution of 3-pyrroline (4.00 g, 57.88 mmol) in MeOH (50 mL), acetic anhydride (23.64 g, 231.56 mmol) was added dropwise. The clear solution was then stirred for 30 min at room temperature, cooled in an ice bath once more, and made alkaline with 2 M aq. NaOH. After extraction with dichloromethane (3 × 100 mL), the combined organic phases were dried with Na_2SO_4 and concentrated to dryness. The oily residue was sublimed (10^{-2} mbar, 40 °C) to yield 1-acetyl-3-pyrroline as white crystals (6.07 g, 94%). – C_6H_9NO (111.1): calcd. C 64.84, H 8.16, N 12.60; found C 64.92, H 8.41, N 12.51. – ^1H NMR ($CDCl_3$): $\delta = 2.08$ (s, 3 H), 4.25 (m, 4 H), 5.81 (m, 1 H), 5.88 (m, 1 H). – $^{13}C\{^1H\}$ NMR ($CDCl_3$): $\delta = 22.1$ (CH_3), 52.8 (CH_2), 54.2 (CH_2), 125.0 (CH), 126.5 (CH), 169.1 (C).

1-Acetyl-*cis*-3,4-pyrrolidinediol: 1-Acetyl-3-pyrroline (8.93 g, 80.35 mmol) and 4-methylmorpholine 4-oxide monohydrate (12.99 g, 96.11 mmol) were dissolved in acetone/H_2O (1:1, v/v; 160 mL). A solution of OsO_4 (2.5% in *tert*-butyl alcohol; 1 mL) was added and the pale-yellow solution was stirred for 24 h. $Na_2S_2O_5$ (1.5 g) was then added and the mixture was stirred for a further 1 h. It was then acidified to pH = 2 with 50% H_2SO_4 and extracted with CH_2Cl_2 (3 × 100 mL). The aqueous layer was diluted to a total volume of 1000 mL with H_2O and was sorbed onto Dowex 50 W-X2. The resin was washed with H_2O until neutral and the collected eluent was sorbed onto Dowex 2-X8. This second column was rinsed with H_2O and the neutral eluent was concentrated to dryness yielding the diol as a colorless oil, which solidified after drying in vacuo (10.55 g, 90%). – $C_6H_{11}NO_3$ (145.2): calcd. C 49.65, H 7.64, N 9.65; found C 49.65, H 7.84, N 9.64. – ^1H NMR (D_2O): $\delta = 2.05$ (s, 3 H), 3.36 (dd, $J = 4.5$, 12.5 Hz, 1 H), 3.47 (dd, $J = 5.5$, 11.5 Hz, 1 H), 3.61 (dd, $J = 5.5$, 12.5 Hz, 1 H), 3.78 (dd, $J = 6.0$, 11.0 Hz, 1 H), 4.31 (m, 1 H), 4.35 (m, 1 H). – $^{13}C\{^1H\}$ NMR (D_2O): $\delta = 23.8$ (CH_3), 52.6 (CH_2), 54.2 (CH_2), 72.7 (CH), 73.5 (CH), 176.1 (C).

(3*S,4*R**)-1-Acetyl-3,4-pyrrolidinediyl Bis(methanesulfonate):** 1-Acetyl-*cis*-3,4-pyrrolidinediol (4.00 g, 27.56 mmol) was dissolved in dry pyridine (150 mL) and the resulting solution was cooled to –10 °C (ice/NaCl). Methanesulfonyl chloride (4.67 mL, 60.10 mmol) was added dropwise with stirring. The ice bath was removed and

the mixture was stirred for 1 h at room temperature. The suspension was then poured into Et_2O (1000 mL) and the resulting mixture was left to stand for 2 d at 4 °C. The Et_2O was decanted and the remaining white solid was redissolved in hot acetone (150 mL). This solution was subjected to flash chromatography (silica gel/acetone) and the eluate was concentrated to dryness. Yield 7.50 g (90%) of a white solid. − $C_8H_{15}NO_7S_2$ (301.3): calcd. C 31.89, H 5.02, N 4.65; found C 31.80, H 5.01, N 4.60. − ^{1}H NMR ([D$_6$]acetone): δ = 2.01 (s, 3 H), 3.26 (s, 3 H), 3.27 (s, 3 H), 3.62 (dd, *J* = 5.5, 10.0 Hz, 1 H), 3.74 (dd, *J* = 6.0, 11.0 Hz, 1 H), 3.83 (dd. *J* = 5.0, 10.0 Hz), 4.07 (dd, *J* = 6.0, 11.0 Hz, 1 H), 5.38 (m, 1 H), 5.43 (m, 1 H). − ^{13}C{^{1}H} NMR ([D$_6$]acetone): δ = 21.8 (CH_3), 38.5 (CH_3), 38.6 (CH_3), 48.8 (CH_2), 49.9 (CH_3), 77.1 (CH), 77.3 (CH), 169.4 (C).

1-Acetyl-*cis*-3,4-diaminopyrrolidine: A stirred mixture of (3*S**,4*R**)-1-acetyl-3,4-pyrrolidinediyl bis(methanesulfonate) (7.50 g, 24.89 mmol) and NaN_3 (8.10 g, 124.60 mmol) in dry DMF (200 mL) was heated at 100 °C for 4 h. The white solid formed was filtered off and washed with dry DMF (2 × 50 mL). To the dark-red solution was added 10% Pd/C (500 mg) and the suspension was immediately transferred to an autoclave for hydrogenation. A small sample was extracted from the reaction mixture with Et_2O for NMR characterization of the diazide. This sample was set aside, the Et_2O was evaporated, and the oily residue was redissolved in CD_3CN. − ^{1}H NMR (CD_3CN): δ = 1.91 (s, 3 H), 3.28 (dd, *J* = 5.0, 12.5 Hz, 1 H), 3.38 (dd, *J* = 5.5, 11.0 Hz, 1 H), 3.56 (dd, *J* = 5.0, 12.5 Hz, 1 H), 3.77 (dd, *J* = 6.0, 10.5 Hz, 1 H), 4.38 (m, 1 H), 4.43 (m, 1 H). − ^{13}C{^{1}H} NMR (CD_3CN): δ = 22.2 (CH_3), 49.0 (CH_2), 50.3 (CH_2), 62.0 (CH), 63.0 (CH), 171.6 (C). − The main portion of the reaction mixture was hydrogenated with vigorous stirring (room temp., 4 bar) for 12 h and then the mixture was filtered. The clear filtrate was acidified to pH = 2 with 3 M HCl, diluted to a total volume of 1000 mL with H_2O, and sorbed onto Dowex 50 W-X2. The column was washed with H_2O and 0.5 M HCl. Elution with 3 M HCl gave a yellow fraction, which was concentrated to dryness. ^{1}H NMR spectroscopy indicated mainly the formation of 1-acetyl-*cis*-3,4-diaminopyrrolidine (ca. 95%) besides some *cis*-3,4-diaminopyrrolidine (5.00 g of crude product). − ^{1}H NMR of the main component (D_2O; pD < 2): δ = 2.12 (s, 3 H), 3.74 (dd, *J* = 5.5, 13.0 Hz, 1 H), 3.87 (dd, *J* = 6.0, 12.0 Hz, 1 H), 3.94 (dd, *J* = 6.5, 13.0 Hz, 1 H), 4.16 (dd, *J* = 6.5, 12.0 Hz, 1 H), 4.35 (m, 1 H), 4.40 (m, 1 H); (D_2O; pD > 12): δ = 2.06 (s, 3 H), 3.25 (dd, *J* = 5.0, 12.0 Hz, 1 H), 3.35 (dd, *J* = 6.0, 11.0 Hz, 1 H), 3.47 (m, 1 H), 3.51 (m, 1 H), 3.59 (dd, *J* = 6.5, 12.5 Hz, 1 H), 3.76 (dd, *J* = 6.5, 11.0 Hz, 1 H). − ^{13}C{^{1}H} NMR for 1-acetyl-*cis*-3,4-diaminopyrrolidine (D_2O; pD < 2): δ = 24.1 (CH_3), 49.6 (CH_2), 51.0 (CH_2), 52.4 (CH), 53.3 (CH), 176.1 (C); (D_2O; pD > 12): δ = 23.8 (CH_3), 53.5 (CH_2), 54.6 (CH), 55.2 (CH_2), 55.6 (CH), 175.8 (C).

***cis*-3,4-Diaminopyrrolidine:** The crude 1-acetyl-*cis*-3,4-diaminopyrrolidine (7.40 g) was dissolved in 3 M HCl (150 mL) and the solution was heated to 100 °C for 1 h. It was then diluted to a total volume of 2000 mL with H_2O and sorbed onto Dowex 50 W-X2. The column was eluted with H_2O, 0.5 M HCl, and 3 M HCl. The last fraction was collected and concentrated to dryness. The white solid obtained was redissolved in H_2O (50 mL) and reprecipitated with conc. HCl (100 mL). The product was washed with EtOH and Et_2O and dried in air yielding *cis*-dap·3HCl·H_2O (5.37 g, 69%). − $C_4H_{16}Cl_3N_3O$ (228.5): calcd. C 21.02, H 7.06, N 18.39; found C 20.99, H 6.97, N 18.37. − ^{1}H NMR (D_2O; pD < 2): δ = 3.71 (m, 2 H), 3.99 (m, 2 H), 4.41 (m, 2 H); (D_2O; pD > 12): δ = 2.53 (m, 2 H), 3.11 (m, 2 H), 3.23 (m, 2 H). − ^{13}C{^{1}H} NMR (D_2O; pD < 2): δ = 49.4 (CH_2), 52.5 (CH); (D_2O; pD > 12): δ = 53.9 (CH_2), 56.2 (CH). − Single crystals were grown from an aqueous solution by slow evaporation of the water; *cis*-dap·3HNO_3·H_2O was prepared by deprotonation of *cis*-dap·3HCl·H_2O (1.00 g, 4.38 mmol) on Dowex 2-X8 (OH^- form). The alkaline fraction was concentrated to dryness and the residual oil was redissolved in MeOH (50 mL). The resulting solution was acidified with 3 equiv. of HNO_3 (3 M in H_2O) and left to stand at 4 °C for 14 h. The precipitate obtained was collected by filtration and dried in air. Yield 1.12 g (83%). − $C_4H_{16}N_6O_{10}$ (308.2): calcd. C 15.59, H 5.23, N 27.27; found C 15.71, H 5.26, N 26.95.

[Pd(H*cis*-dap)$_2$](ClO$_4$)$_4$·H$_2$O: A mixture of *cis*-dap·3HCl·H_2O (0.40 g, 1.75 mmol) and $PdCl_2$ (0.16 g, 0.87 mmol) in H_2O (50 mL) was refluxed for 3 h and the clear yellow solution was sorbed onto Dowex 2-X8 (OH^- form). The column was washed with H_2O until a neutral eluent was obtained. The combined alkaline fractions were acidified with 70% $HClO_4$ and the solvents were carefully evaporated under reduced pressure until a volume of 5 mL remained. Conc. $HClO_4$ (5 mL) was added and the solution was set aside at room temperature for 2 d. Slightly yellow crystals precipitated. These were collected by filtration and washed with EtOH and Et_2O (0.52 g, 82%). − $C_8H_{26}Cl_4N_6O_{17}Pd$ (726.6): calcd. C 13.22, H 3.61, N 11.57; found C 13.33, H 3.51, N 11.54. − ^{1}H NMR (D_2O; pD < 2): δ = 3.64 (m, 4 H), 3.82 (m, 4 H), 3.95 (m, 4 H); (D_2O; pD > 12): δ = 3.02 (m, 4 H), 3.28 (m, 4 H), 3.60 (m, 4 H). − ^{13}C{^{1}H} NMR (D_2O; pD < 2): δ = 50.8 (CH_2), 50.9 (CH_2), 62.4 (CH), 62.5 (CH); (D_2O; pD > 12): δ = 52.5 (CH_2), 52.6 (CH_2), 63.9 (CH), 64.0 (CH). − UV/Vis: λ_{max} (ε) = 290 (347). − Crystals were grown by slow evaporation of the water from an aqueous solution of [Pd(H*cis*-dap)$_2$](ClO$_4$)$_4$ that had been acidified with a few drops of $HClO_4$.

[Pt(H*cis*-dap)Cl$_4$]Cl·H$_2$O: *cis*-dap·3HCl·H_2O (250 mg, 1.09 mmol) was dissolved in H_2O (10 mL) and deprotonated using Dowex 2-X8 (OH^- form). The resulting solution was then concentrated to dryness under reduced pressure. The oily residue was redissolved in dry EtOH (5 mL) and this solution was cooled to 0 °C. A solution of H_2PtCl_6·$6H_2O$ (283 mg, 0.55 mmol) in dry EtOH (10 mL) was then added dropwise, which led to the deposition of a yellow precipitate. The suspension was stirred for 2 h at 65 °C. The solid was then collected by filtration, recrystallized from hot H_2O (3 mL) and conc. HCl (20 mL), and washed with EtOH and Et_2O. Yellow powder (150 mg, 55%). − $C_4H_{14}Cl_5N_3OPt$ (492.5): calcd. C 9.75, H 2.87, N 8.53; found C 10.16, H 2.89, N 8.68. − ^{1}H NMR (D_2O; pD < 2): δ = 3.96 (m, 4 H), 4.38 (m, 2 H). − ^{13}C{^{1}H} NMR (D_2O; pD < 2): δ = 48.9 (CH_2), 66.2 (CH).

[Cu(H*cis*-dap)$_2$(OH$_2$)$_2$](SO$_4$)·3.5H$_2$O: *cis*-dap·3HCl·H_2O (250 mg, 1.09 mmol) was dissolved in H_2O (10 mL) and deprotonated using Dowex 2-X8 (OH^- form). The resulting solution was concentrated to dryness under reduced pressure and the oily residue was redissolved in MeOH (50 mL). A solution of $CuSO_4$·$5H_2O$ (272 mg, 1.09 mmol) in H_2O (5 mL) was added, which led to the deposition of a blue precipitate. The suspension was diluted with H_2O (10 mL) and refluxed for 1 h. The insoluble solid was then removed by filtration. MeOH was added dropwise to the deep-blue solution until it became turbid. Single crystals were grown by heating the suspension until the precipitate redissolved and then allowing it to slowly cool to room temperature. − $C_8H_{35}CuN_6O_{13.5}S_2$ (559.1): calcd. C 17.19, H 6.31, N 15.03; found C 17.00, H 6.19, N 14.89.

[Co(*cis*-dap)(tach)]Cl$_3$·1.5H$_2$O: *cis*-dap·3HCl·H_2O (241 mg, 1.05 mmol) was dissolved in H_2O (10 mL) and deprotonated using Dowex 2-X8 (OH^- form). The resulting solution was concentrated to dryness under reduced pressure and the oily residue was redis-

solved in dry MeOH (50 mL). This solution was added dropwise to a purple solution of [Co(tach)$(NO_3)_3$] (3.16 mmol) in dry MeOH. The mixture was refluxed for 14 h and then concentrated to dryness. The brownish residue was suspended in H_2O (30 mL) and the suspension was acidified with 3 M HCl and heated to boiling for a few minutes. Insoluble components were removed by filtration. The orange-red filtrate was diluted to a volume of 500 mL with H_2O and sorbed onto Dowex 50 W-X2. The column was eluted with 0.5 M HCl to give a pink fraction, which was discarded. Further elution with 3 M HCl gave an orange fraction, which was concentrated to dryness. Recrystallization from 6 M HCl yielded 65 mg (14%) of the trichloride salt. – $C_{10}H_{29}CoCl_3N_6O_{1.5}$ (422.7): calcd. C 28.42, H 6.92, N 19.88; found C 28.41, H 6.68, N 19.75. – ^{1}H NMR (D_2O): δ = 1.88 (m, 3 H), 2.14 (m, 3 H), 2.60 (d, J = 11.0 Hz, 2 H), 2.79 (d, J = 11.0 Hz, 2 H), 2.84 (s, 1 H), 3.09 (s, 2 H), 3.78 (s, 2 H). – ^{13}C{^{1}H} NMR: δ = 33.6 (CH_2), 33.7 (CH_2), 42.4 (CH), 42.7 (CH), 59.3 (CH), 62.6 (CH_2). – UV/Vis: λ_{max} (ε) = 351 (142), 475 (102). – CV: E = −210 mV. – Crystals of the chloride tetrachlorozincate salt suitable for X-ray diffraction analysis were grown by layering a solution of [Co(*cis*-dap)(tach)]Cl_3 and $ZnCl_2$ in conc. HCl with EtOH at 4 °C.

***trans*-(3*R*,4*R*)-Diaminopyrrolidine:** A mixture of (3*S*,4*S*)-1-benzyl-3,4-pyrrolidinediyl bis(methanesulfonate) (11.9 g, 34.06 mmol) and NaN_3 (5.2 g, 80.00 mmol) in dry DMF (150 mL) was stirred at 100 °C for 4 h. After cooling to room temperature, the white solid was filtered off and the resulting solution was subjected to hydrogenation in a two-step procedure. (1) Reduction of the diazide: The solution was transferred into an autoclave and hydrogenated for 12 h at 4 bar in the presence of 10% Pd/C (500 mg) under vigorous stirring. The catalyst was removed by filtration. The filtrate was acidified with 3 M HCl and concentrated to dryness. The brownish residue was redissolved in H_2O (250 mL) and sorbed onto Dowex 50 W-X2. The column was washed with H_2O and eluted with HCl (0.5 M, 3.0 M, 6.0 M; 500 mL each). The latter two fractions were combined and concentrated to dryness. (2) Cleavage of the benzyl group: The product was taken up in a mixture of MeOH (100 mL), H_2O (50 mL), and acetic acid (20 mL) and the suspension was again hydrogenated in an autoclave for 12 h at 4 bar in the presence of 10% Pd/C (400 mg). The catalyst was removed and the clear solution was concentrated to dryness. The solid was then suspended in refluxing conc. HCl (100 mL) and small portions of H_2O were added until complete dissolution. After cooling to room temperature, the product was precipitated by adding EtOH (50 mL), collected by filtration, washed with EtOH and Et_2O, and dried in vacuo. White crystals of the composition *trans*-(3*R*,4*R*)-dap·3HCl·0.25H_2O were obtained (3.32 g, 45%). – $C_4H_{14.5}Cl_3N_3O_{0.25}$ (215.0): calcd. C 22.34, H 6.80, N 19.54; found C 22.25, H 6.82, N 19.54. – ^{1}H NMR (D_2O; pD < 2): δ = 3.70 (dd, J = 8.0, 10.0 Hz, 2 H), 4.12 (dd, J = 7.0, 10.0 Hz, 2 H), 4.42 (m, 2 H); (D_2O; pD > 12): δ = 2.53 (dd, J = 5.0, 10.0 Hz, 2 H), 3.02 (m, 2 H), 3.15 (dd, J = 6.0, 10.0 Hz, 2 H). – ^{13}C{^{1}H} NMR (D_2O; pD < 2): δ = 50.0 (CH_2), 54.6 (CH); (D_2O; pD > 12): δ = 54.9 (CH_2), 62.1 (CH). – Single crystals of *trans*-(3*R*,4*R*)-dap·3HCl·0.5H_2O were grown from an aqueous solution by slow evaporation of the water.

(1*S,2*R**)-1,2-Cyclopentanediyl Bis(methanesulfonate):** A solution of *cis*-1,2-cyclopentanediol (2.50 g, 24.48 mmol) in dry pyridine (50 mL) was cooled to 0 °C in an ice/NaCl bath. Methanesulfonyl chloride (3.89 mL, 50.00 mmol) was then added dropwise. A white precipitate appeared. The ice bath was removed and the solution was stirred at room temperature for 1 h and then cooled to 0 °C once more. Excess pyridine was neutralized by the addition of 3 M HCl (200 mL) in small portions whilst stirring. The product precipitated as a white solid, which was collected by filtration, washed with H_2O, and dried in vacuo (5.23 g, 83%). – $C_7H_{14}O_6S_2$ (258.31): calcd. C 32.55, H 5.46; found C 32.42, H 5.31. – ^{1}H NMR ($CDCl_3$): δ = 1.67–1.73 (m, 1 H), 1.98–2.12 (m, 5 H), 3.10 (s, 6 H), 5.00 (m, 2 H). – ^{13}C{^{1}H} NMR ($CDCl_3$): δ = 18.3 (CH_2), 28.4 (CH_2), 38.5 (CH_3), 80.5 (CH).

***cis*-1,2-Diaminocyclopentane:** A mixture of (1*S**,2*R**)-1,2-cyclopentanediyl bis(methanesulfonate) (4.49 g, 17.38 mmol) and NaN_3 (3.40 g, 53.30 mmol) was heated at 100 °C whilst stirring in dry DMF (100 mL) for 4 h and then stirred for an additional 12 h at room temperature. H_2O (100 mL) was then added and the mixture was extracted with Et_2O (4 × 100 mL). The combined ethereal phases were washed with H_2O (100 mL) and dried with Na_2SO_4. A small sample (5 mL) was set aside until the ether evaporated, and the oily residue was dissolved in $CDCl_3$ for NMR characterization of the diazide. – ^{1}H NMR ($CDCl_3$): δ = 1.60–1.68 (m, 1 H), 1.76–1.94 (m, 5 H), 3.80 (m, 2 H). – ^{13}C{^{1}H} NMR ($CDCl_3$): δ = 19.9 (CH_2), 27.9 (CH_2), 64.4 (CH). – The main portion of the ethereal solution was concentrated under reduced pressure to a volume of 200 mL and then diluted with EtOH (150 mL). This solution was transferred to an autoclave and hydrogenated for 26 h at 4 bar under vigorous stirring in the presence of 10% Pd/C (300 mg). The resulting suspension was heated to boiling for a few minutes and the catalyst was removed by filtration. The clear filtrate was concentrated under reduced pressure to a volume of 150 mL. Conc. HCl was added portionwise until the product precipitated (white needles). The solid was collected by filtration, washed with EtOH, and equilibrated in air, yielding *cis*-cptn·2HCl·0.5H_2O (1.57 g; 50% based on the amount of methanesulfonate). – $C_5H_{15}Cl_2N_2O_{0.5}$ (182.1): calcd. C 32.98, H 8.30, N 15.38; found C 33.00, H 8.30, N 15.35. – ^{1}H NMR (D_2O; pD < 2): δ = 1.80–1.93 (m, 3 H), 1.94–2.00 (m, 1 H), 2.23 (m, 2 H), 3.92 (m, 2 H); (D_2O; pD > 12): δ = 1.38 (m, 2 H), 1.52 (m, 1 H), 1.70 (m, 1 H), 1.86 (m, 2 H), 3.07 (m, 2 H). – ^{13}C{^{1}H} NMR (D_2O; pD < 2): δ = 21.7 (CH_2), 29.8 (CH_2), 55.6 (CH); (D_2O; pD > 12): δ = 22.7 (CH_2), 33.7 (CH_2), 57.3 (CH).

[Ni(*cis*-cptn)$_2$](ClO_4)$_2$: *cis*-cptn·2HCl·0.5H_2O (200 mg, 0.99 mmol) was dissolved in H_2O (10 mL) and deprotonated using Dowex 2-X8 (OH^- form). The resulting solution was concentrated to dryness under reduced pressure and the oily residue was redissolved in dry MeOH (100 mL). A solution of $Ni(ClO_4)_2$·6H_2O (183 mg, 0.50 mmol) in dry MeOH (25 mL) was added. The resulting yellow solution was stored at 4 °C for 14 h. Yellow crystals suitable for X-ray diffraction studies precipitated. These were collected by filtration and dried in air (227 mg, 85%). – $C_{10}H_{24}Cl_2N_4NiO_8$ (457.9): calcd. C 26.23, H 5.28, N 12.24; found C 26.24, H 5.26, N 12.21. – UV/Vis: λ_{max} (ε) = 357 (8.8), 444 (8.3), 574 (5.3).

(1*R,2*R**)-1,2-Cyclopentanediyl Bis(methanesulfonate):** Racemic *trans*-1,2-cyclopentanediol (1.86 g, 18.21 mmol) was converted into the bis(methanesulfonate) as described above for the *cis* isomer. Yield 2.71 g (58%). – $C_7H_{14}O_6S_2$ (258.3): calcd. C 32.55, H 5.46; found C 32.46, H 5.19. – ^{1}H NMR ($CDCl_3$): δ = 1.87 (quint, J = 7.0 Hz, 2 H), 1.91–1.97 (m, 2 H), 2.22 (m, 2 H), 3.07 (s, 6 H), 5.08 (m, 2 H). – ^{13}C{^{1}H} NMR ($CDCl_3$): δ = 20.9 (CH_2), 30.5 (CH_2), 38.4 (CH_3), 84.8 (CH).

***trans*-1,2-Diaminocyclopentane:** A mixture of (1*R**,2*R**)-1,2-cyclopentanediyl bis(methanesulfonate) (2.71 g, 10.49 mmol) and NaN_3 (2.05 g, 31.53 mmol) in dry DMF (100 mL) was allowed to react and then hydrogenated as described above for the *cis* isomer. The catalyst was removed by filtration, and the filtrate was acidified

with 3 M HCl and concentrated to dryness. The residue was redissolved in H_2O (1000 mL) and sorbed onto Dowex 50 W-X2. The column was eluted with H_2O and aqueous HCl (0.5 M and 3.0 M; 500 mL each). The last fraction was concentrated to dryness and the residual white solid was dried in vacuo (1.13 g, 62%). − $C_5H_{14}Cl_2N_2$ (173.1): calcd. C 34.70, H 8.15, N 16.18; found C 34.73, H 8.03, N 16.09. − ^{1}H NMR (D_2O; pD < 2): δ = 1.83 (m, 2 H), 1.89 (quint, J = 7.0 Hz, 2 H), 2.32 (m, 2 H), 3.81 (m, 2 H); (D_2O; pD > 12): δ = 1.32 (m, 2 H), 1.64 (quint, J = 8.0 Hz, 2 H), 1.95 (m, 2 H), 2.77 (m, 2 H). − ^{13}C{^{1}H} NMR (D_2O; pD < 2): δ = 24.5 (CH_2), 32.5 (CH_2), 58.0 (CH); (D_2O; pD > 12): δ = 22.8 (CH_2), 34.9 (CH_2), 62.4 (CH).

[Cu(3*R*-ampy)(3*S*-ampy)](ClO$_4$)$_2$: Racemic ampy·2HCl (1.75 g, 11.19 mmol) was dissolved in H_2O (10 mL) and deprotonated using Dowex 2-X8 (OH^- form). The resulting solution was concentrated to dryness under reduced pressure and the oily residue was redissolved in dry EtOH (50 mL). A solution of $Cu(ClO_4)_2·6H_2O$ (1.85 g, 4.99 mmol) in dry EtOH (25 mL) was added dropwise. The blue precipitate was collected by filtration, washed with Et_2O, and dried in air (1.75 g, 81%). − $C_8H_{20}Cl_2CuN_4O_8$ (434.7): calcd. C 22.10, H 4.64, N 12.89; found C 21.76, H 4.56, N 12.81. − UV/Vis: λ_{max} (ε) = 554 (127). − Single crystals were grown by slow cooling of a hot saturated solution of $[Cu(ampy)_2](ClO_4)_2$ in MeOH.

Potentiometric Measurements: Potentiometric titrations were carried out with a Metrohm 713 pH/mV meter and a Metrohm combined glass electrode with an internal Ag/AgCl reference.[5,14] The sample solutions were titrated with 0.1 M or 1.0 M KOH using a Metrohm 665 piston burette. Addition of the titrant and the pH meter reading were controlled using an in-house computer program and a PC. The ionic strength of each 50-mL sample solution was 0.1 mol dm^{-3} KCl, 0.1 mol dm^{-3} KNO_3, or 1.0 mol dm^{-3} KNO_3 and the stability of the electrode was checked by calibration titrations prior to and after each measurement. All titrations were performed at 25.0 °C under nitrogen (scrubbed with an aqueous solution of the inert electrolyte). To determine the pK_a values of the ligands, several alkalimetric titrations were carried out with analytically pure samples of the corresponding hydrochlorides. Test solutions for the titration experiments were prepared using the solid hydrochlorides (*cis*-dap·3HCl, *cis*-cptn·2HCl, *trans*-cptn·2HCl) or a stock solution (ampy·2HCl), standardized aqueous stock solutions of the metal chlorides (Cu, Ni, Zn), or solid $Cd(NO_3)_2·4H_2O$. Complete equilibration was ensured by performing acidimetric back titrations (with 0.1 mol dm^{-3} HCl or 0.1 mol dm^{-3} HNO_3). The data were only considered reliable when no significant hysteresis was observed.

Spectrophotometric Titrations: The titrations were carried out as described in the previous section (50 mL sample solution, 0.01−0.02 mol dm^{-3} total Cu, 1 mol dm^{-3} KNO_3, 25.0 ± 0.1 °C). Additionally, the titration cell was equipped with an immersion probe (HELLMA), which was connected to a diode-array spectrophotometer (J & M, TIDAS-UV/NIR/100−1). An in-house computer program was used to control the addition of the titrant (1 mol dm^{-3} KOH). This program allowed a sample spectrum to be recorded prior to each addition of an aliquot of the titrant.

Calculation of the Equilibrium Constants: All equilibrium constants were calculated as concentration constants and pH was defined as −log [H^+]. The pK_a values of the ligands and the formation constants of the complexes were calculated using the computer program HYPERQUAD.[36] All equilibrium constants were evaluated with fixed values for the total concentrations of the reactants and for pK_w (13.78 for μ = 0.1 mol dm^{-3}, 13.71 for μ = 1.0 mol dm^{-3}).[26] For the refinement of the formation constants of the metal complexes, fixed values were used for the protonation con-

Table 7. Crystallographic data for H$_3$*cis*-dapCl$_3$·H$_2$O and H$_3$*trans*-dapCl$_3$·0.5H$_2$O

Compound	H$_3$*cis*-dapCl$_3$·H$_2$O	H$_3$*trans*-dapCl$_3$·0.5H$_2$O
Empirical formula	$C_4H_{16}Cl_3N_3O$	$C_4H_{14}Cl_3N_3O_{0.5}$
Molecular mass	228.55	218.53
Temperature [K]	293(2)	293(2)
Crystal system	monoclinic	orthorhombic
Space group	$P2_1$	$P2_12_12$
a [Å]	6.3903(7)	12.476(2)
b [Å]	11.4227(13)	12.783(3)
c [Å]	7.4879(9)	6.4860(10)
β [°]	114.969(7)	90.00
V [Å^3]	495.49(10)	1034.4(3)
Z	2	4
$D_{calcd.}$ [g cm^{-3}]	1.532	1.403
μ [mm^{-1}]	0.880	0.837
F[000]	240	456
Crystal size [mm]	0.30 × 0.35 × 0.20	0.50 × 0.45 × 0.35
θ min. and max.	5.51 to 27.50	2.28 to 24.02
Data set	−8/8; −14/14; −9/9	−14/14; −13/13; −7/7
Transmission, min. and max.	not measured	not measured
Total data, unique data	4510, 2261	6274, 1493
Reflections with $I > 2\sigma(I)$	2048	1483
Parameters/restraints	149/9	152
R_1, wR_2 [$I > 2\sigma(I)$]	0.0266, 0.0527	0.0251, 0.0696
R_1, wR_2 (all data)	0.0332, 0.0542	0.0253, 0.0698
Largest peak/hole [e/Å^3]	0.224 and −0.204	0.454 and −0.149
Max. shift/error	0.006	0.005

Table 8. Crystallographic data for $[Pd(H\textit{cis}\text{-dap})_2](ClO_4)_4\cdot 2H_2O$, $[Pt(H\textit{cis}\text{-dap})Cl_4]Cl\cdot H_2O$, $[Co(\textit{cis}\text{-dap})(tach)][ZnCl_4]Cl\cdot C_2H_5OH$, $[Ni(\textit{cis}\text{-cptn})_2](ClO_4)_2$, and $[Cu(ampy)_2](ClO_4)_2$

Compound	$[Pd(H\textit{cis}\text{-dap})_2](ClO_4)_4\cdot 2H_2O$	$[Pt(H\textit{cis}\text{-dap})Cl_4]Cl\cdot H_2O$	$[Co(\textit{cis}\text{-dap})(tach)][ZnCl_4]Cl\cdot EtOH$	$[Ni(\textit{cis}\text{-cptn})_2](ClO_4)_2$	$[Cu(ampy)_2](ClO_4)_2$
Empirical formula	$C_8H_{28}Cl_4N_6O_{18}Pd$	$C_4H_{14}Cl_5N_3OPt$	$C_{12}H_{32}Cl_5CoN_6OZn$	$C_{10}H_{24}Cl_2N_4NiO_8$	$C_8H_{20}Cl_2CuN_4O_8$
Molecular mass	744.56	492.52	577.99	457.94	434.72
Temperature [K]	293(2)	298(2)	233(2)	293(2)	213(2)
Crystal system	monoclinic	orthorhombic	monoclinic	monoclinic	monoclinic
Space group	$P2_1/c$	$Pc2_1b$	$P2_1/c$	$C2/c$	$P2_1$
a [Å]	9.8381(15)	7.984(3)	8.0147(12)	22.450(4)	8.633(3)
b [Å]	12.6413(19)	11.210(3)	18.527(3)	7.605(2)	10.789(3)
c [Å]	9.9609(15)	14.271(5)	15.440(2)	12.016(2)	8.850(4)
β [°]	104.93(3)	90.00	93.5(5)	116.68(3)	110.41(4)
V [Å^3]	1197.0(3)	1277.3(7)	2288.3(6)	1833.1(7)	772.5(5)
Z	2	4	4	4	2
$D_{calcd.}$ [g cm^{-3}]	2.066	2.561	1.678	1.659	1.869
μ [mm^{-1}]	1.317	12.006	2.372	1.395	1.807
F[000]	752	920	1184	952	446
Crystal size [mm]	0.76 × 0.34 × 0.31	0.46 × 0.46 × 0.27	0.46 × 0.10 × 0.10	0.50 × 0.45 × 0.30	0.65 × 0.63 × 0.04
Transm. coeff.	0.4342, 0.6855	0.0139, 0.0578	0.4084, 0.7974	not measured	0.445, 1.000
θ min. and max.	2.14 to 33.08	1.81 to 30.00	1.72 to 28.33	2.86 to 25.82	2.84 to 25.00
Data set	−15/10; −18/15; −14/14	−11/11; −15/15; −20/20	−10/7; −23/24; −20/20	−27/27; −8/8; −14/14	−8/10; −7/12; −8/10
Total data, unique data	12170, 4107	4326, 2260	19108, 5691	6637, 1672	1880, 1587
Reflns. with $I > 2\sigma(I)$	3295	2043	3725	1161	1554
Parameters/restraints	225/2	146/2	343/0	194/0	208/1
R_1, wR_2 [$I > 2\sigma(I)$]	0.0389, 0.1078	0.0419, 0.1088	0.0450, 0.0980	0.0423, 0.0947	0.0375, 0.0933
R_1, wR_2 (all data)	0.0508, 0.1153	0.0465, 0.1127	0.0785, 0.1076	0.0652, 0.1023	0.0386, 0.0940
Max. peak/hole [e/Å^3]	1.308/−0.914	1.998/−2.092	0.829/−1.233	0.430/−0.458	0.571/−0.836
Max. shift/error	0.014	0.000	0.008	0.000	0.000

Table 9. Crystallographic data for $[Cu(H\textit{cis}\text{-dap})_2(OH_2)_2](SO_4)_2\cdot 3.5H_2O - 2x\ H^+ + x\ Cu^{2+}$

Compound	$x < 0.01$	$x = 0.08$	$x = 0.11$
Empirical formula	$C_8H_{35}CuN_6O_{13.5}S_2$	$C_8H_{34.84}Cu_{1.08}N_6O_{13.5}S_2$	$C_8H_{34.78}Cu_{1.11}N_6O_{13.5}S_2$
Molecular mass	559.08	563.99	565.54
Temperature [K]	100(2)	293(2)	293(2)
Crystal system	orthorhombic	orthorhombic	orthorhombic
Space group	*Pccn*	*Pccn*	*Pccn*
a [Å]	24.635(2)	24.670(5)	24.703(5)
b [Å]	13.1027(12)	13.110(3)	13.115(3)
c [Å]	13.4177(12)	13.417(3)	13.479(3)
V [Å^3]	4331.0(7)	4339.4(16)	4366.9(17)
Z	8	8	8
$D_{calcd.}$ [g cm^{-3}]	1.715	1.727	1.720
μ [mm^{-1}]	1.277	1.353	1.366
F[000]	2353	2369	2375
Crystal size [mm]	0.58 × 0.48 × 0.16	0.3 × 0.25 × 0.1	0.25 × 0.20 × 0.10
Transm. coeff.	0.485, 0.753	not measured	not measured
θ min. and max.	1.76 to 33.00	1.65 to 24.02	2.32 to 26.04
Data set	−22/37; −20/19; −20/18	0/28; 0/15; 0/15	−28/29; −16/16; −16/16
Total data, unique data	44850, 8148	3407, 3407	32097, 4157
Reflns. with $I > 2\sigma(I)$	6386	2854	2484
Parameters/restraints	323/61	284/0	284/0
R_1, wR_2 [$I > 2\sigma(I)$]	0.0356, 0.0839	0.0546, 0.1446	0.0694, 0.1164
R_1, wR_2 (all data)	0.0535, 0.0918	0.0662, 0.1567	0.1325, 0.1514
Max. peak/hole [e/Å^3]	1.578/−0.371	0.603/−1.508	0.810/−0.464
Max. shift/error	0.001	0.000	0.000

stants of the ligands, as obtained from the pK_a determinations. The spectrophotometric measurements were evaluated using the computer program SPECFIT.[37,38] The spectrum of free Cu^{2+} was measured separately and was not refined. The free ligands and their protonation products were considered as colorless.

Crystal Structure Determination:[39] X-ray diffraction data were collected with the following diffractometers: STOE IPDS [protonated ligands, Ni complex, Cu(*cis*-dap) complexes with $x = 0.08$, 0.11], STOE STADI-4 (Pt complex), Nonius Kappa-CCD [Cu(*cis*-dap) complex with $x < 0.01$], Siemens SMART PLATFORM (Co complex, Pd complex), Siemens P4 four-circle diffractometer [Cu(ampy) complex]. The crystallographic data are compiled in Tables 7, 8 and 9. Graphite-monochromated Mo-K_α radiation (λ = 0.71073 Å) was used throughout. Low-temperature measurements at 233(2), 213(2), and 100(2) K were performed on the Co complex, the Cu(ampy) complex, and the Cu(*cis*-dap) complex with $x <$ 0.01, respectively. The data for all the other compounds were collected at ambient temperature. Standard reflections were monitored during the data collections. The standard reflections of the Pt complex and $[Cu(ampy)_2](ClO_4)_2$ decreased by 6.2% and 2%, respectively, during the measurements, and decay corrections were applied accordingly. All data sets were corrected for Lorentz and polarization effects. Absorption corrections were applied to the data for the Cu(*cis*-dap) complex with $x < 0.01$ (face-indexed numerical), the Pt complex (empirical with ψ-scans), the Cu(ampy) complex (empirical with DIFABS), and the Co and Pd complexes (empirical with SADABS). The structure of the Pt complex was solved by the heavy atom method; all other structures were solved by direct methods.[40] All structures were refined by full-matrix least-squares techniques[41] against F^2. One of the SO_4^{2-} counterions of the Cu(*cis*-dap) complex with $x > 0.01$ proved to be disordered. These anions exhibited two split positions for one of the oxygen atoms, which were refined with occupancies of 50% each. Non-hydrogen atoms were refined with anisotropic displacement parameters, except for the disordered oxygen positions (O32A, O32B) of the SO_4^{2-} counterions. In general, the positions of the hydrogen atoms were calculated (riding model with $U_{iso} = 1.2 \times U_{eq}$ of the bonded heavy atom), with the exception of the H_2O hydrogen atoms of H$_3$*trans*-dapCl$_3$·0.5H$_2$O, [Pt(H*cis*-dap)Cl$_4$]Cl·H$_2$O, and the Cu(*cis*-dap) complex with $x = 0.08$ and $x = 0.11$, which were not considered. All other hydrogen atoms of H$_3$*trans*-dapCl$_3$·0.5H$_2$O, all H(−N) and H(−O) hydrogen atoms of H$_3$*cis*-dapCl$_3$·H$_2$O, all hydrogen atoms of the Ni and Pd complexes (including H_2O), and the hydrogen atoms of the cation $[Co(cis\text{-dap})(tach)]^{3+}$, together with the OH hydrogen atom of EtOH, were located and refined with variable isotropic displacement parameters. The H(−N) atoms of the coordinated amino groups of [Pt(H*cis*-dap)Cl$_4$]Cl·H$_2$O were placed in calculated positions and were refined with $U_{iso} = 1.2 \times U_{eq}$. The positions of the hydrogen atoms of the noncoordinating ammonium groups and of all the H_2O molecules of the Cu(*cis*-dap) complex with $x = 0.005$ were located and refined isotropically with common bond lengths (0.775 ± 0.005 Å for H−O and 0.855 ± 0.005 Å for H−N). The small amount of additional Cu in this particular specimen (1.5 eÅ^{-3}, $x < 0.01$) was not considered in the refinement. The structures of H$_3$*cis*-dapCl$_3$·H$_2$O, H$_3$*trans*-dapCl$_3$·0.5H$_2$O, and [Pt(H*cis*-dap)Cl$_4$]Cl·H$_2$O were solved and refined in polar space groups. Their absolute structure parameters were refined to values of −0.03(6), −0.01(9), and −0.041(14), respectively.[42] The structure of $[Cu(ampy)_2](ClO_4)_2$ proved to be a racemic twin.

Molecular Modeling Calculations: Molecular modeling calculations were carried out using the commercially available program MOMEC97.[30]

Acknowledgments

We thank Anton Zaschka, Dr. Anja Zimmer, Dr. Volker Huch, Prof. Dr. Michael Veith (all Saarbrücken) and Dr. Peter Osvath (Melbourne) for valuable help and fruitful suggestions. The structure of $[Cu(cis\text{-cptn})_2](ClO_4)_2$ [18] was solved and refined by Manuela Winter (Bochum). Financial support from the Studienstiftung des Deutschen Volkes (D. K.) and the Fonds der Chemischen Industrie (K. H.) is gratefully acknowledged.

[1] A. E. Martell, R. D. Hancock, *Metal Complexes in Aqueous Solutions*, Plenum Press, New York, **1996**.
[2] P. Chaudhuri, K. Wieghardt, *Prog. Inorg. Chem.* **1987**, *35*, 329.
[3] K. Hegetschweiler, *Chem. Soc. Rev.* **1999**, *28*, 239.
[4] H. Manohar, D. Schwarzenbach, W. Iff, G. Schwarzenbach, *J. Coord. Chem.* **1979**, *8*, 213.
[5] J. W. Pauly, J. Sander, D. Kuppert, M. Winter, G. J. Reiß, F. Zürcher, R. Hoffmann, T. F. Fässler, K. Hegetschweiler, *Chem. Eur. J.* **2000**, *6*, 2830.
[6] H. C. Wormser, *J. Pharm. Sci.* **1969**, *58*, 1038.
[7] D. R. Reddy, E. R. Thornton, *J. Chem. Soc., Chem. Commun.* **1992**, 172.
[8] J. Skarzewski, A. Gupta, *Tetrahedron: Asymmetry* **1997**, *8*, 1861.
[9] D. Cremer, J. A. Pople, *J. Am. Chem. Soc.* **1975**, *97*, 1354.
[10] H. Toftlund, E. Pedersen, *Acta Chem. Scand.* **1972**, *26*, 4019.
[11] G. W. H. Potter, M. W. Coleman, A. M. Monro, *J. Heterocycl. Chem.* **1975**, *12*, 611.
[12] S. Ongeri, D. J. Aitken, H.-P. Husson, *Synth. Commun.* **2000**, *30*, 2593.
[13] D. Kuppert, C. Roth, J. Sander, K. Hegetschweiler, *Z. Kristallogr. NCS* **2001**, *216*, 111.
[14] A. Zimmer, D. Kuppert, T. Weyhermüller, I. Müller, K. Hegetschweiler, *Chem. Eur. J.* **2001**, *7*, 917.
[15] E. Prenesti, P. G. Daniele, M. Prencipe, G. Ostacoli, *Polyhedron* **1999**, *18*, 3233.
[16] J. Bjerrum, B. V. Agarwala, *Acta Chem. Scand., Ser. A* **1980**, *34*, 475.
[17] B. J. Hathaway, *J. Chem. Soc., Dalton Trans.* **1972**, 1196.
[18] A low-quality single-crystal X-ray diffraction study of $[Cu(cis\text{-cptn})_2](ClO_4)_2$ confirmed the square-planar (*trans*) CuN_4 geometry: $P\bar{1}$, a = 5.999(1) Å, b = 7.758(2) Å, c = 9.751(3) Å, α = 81.67(2)°, β = 86.83(3)°, γ = 82.71(2)°, $Z = 1$ for $C_{10}H_{24}Cl_2CuN_4O_8$, $R = 0.089$ for 1138 observed reflections [$I > 2\sigma(I)$] and 116 parameters, $wR_2 = 0.210$ for all 1534 unique reflections. The average Cu−N bond length is 2.00 Å.
[19] A. F. Wells, *Structural Inorganic Chemistry*, 5th ed., Clarendon Press, Oxford, **1984**.
[20] P. Comba, A. F. Sickmüller, *Inorg. Chem.* **1997**, *36*, 4500.
[21] P. Hendry, A. Ludi, *Adv. Inorg. Chem.* **1990**, *35*, 117.
[22] P. D. Newman, M. B. Hursthouse, K. M. Abdul Malik, *J. Chem. Soc., Dalton Trans.* **1999**, 599.
[23] C. J. Andres, P. H. Lee, T. H. Nguyen, A. I. Meyers, *J. Org. Chem.* **1995**, *60*, 3189.
[24] A. Corruble, J.-Y. Valnot, J. Maddaluno, Y. Prigent, D. Davoust, P. Duhamel, *J. Am. Chem. Soc.* **1997**, *119*, 10042.
[25] L. Doms, L. Van den Enden, H. J. Geise, C. Van Alsenoy, *J. Am. Chem. Soc.* **1983**, *105*, 158.
[26] R. M. Smith, A. E. Martell, R. J. Motekaitis, *Critically Selected Stability Constants of Metal Complexes*, NIST Standard Reference Database 46, Version 5.0, USA, **1998**.
[27] A. Zimmer, I. Müller, G. J. Reiß, A. Caneschi, D. Gatteschi, K. Hegetschweiler, *Eur. J. Inorg. Chem.* **1998**, 2079.
[28] M. Weber, D. Kuppert, K. Hegetschweiler, V. Gramlich, *Inorg. Chem.* **1999**, *38*, 859.
[29] A. Ringbom, *J. Chem. Educ.* **1958**, *35*, 282.
[30] P. Comba, T. W. Hambley, N. Okon, G. Lauer, *MOMEC: A*

Molecular Modeling Package for Inorganic Compounds, Heidelberg, **1997**.
[31] P. Comba, A. F. Sickmüller, *Angew. Chem.* **1997**, *109*, 2089; *Angew. Chem. Int. Ed. Engl.* **1997**, *36*, 2006.
[32] J. E. Sarneski, A. T. McPhail, K. D. Onan, L. E. Erickson, C. N. Reilley, *J. Am. Chem. Soc.* **1977**, *99*, 7376.
[33] J. S. Warmus, G. J. Dilley, A. I. Meyers, *J. Org. Chem.* **1993**, *58*, 270.
[34] U. Nagel, E. Kinzel, J. Andrade, G. Perscher, *Chem. Ber.* **1986**, *119*, 3326.
[35] L. Hausherr-Primo, K. Hegetschweiler, H. Rüegger, L. Odier, R. D. Hancock, H. W. Schmalle, V. Gramlich, *J. Chem. Soc., Dalton Trans.* **1994**, 1689.
[36] P. Gans, A. Sabatini, A. Vacca, *Talanta* **1996**, *43*, 1739.
[37] R. A. Binstead, B. Jung, A. D. Zuberbühler, *SPECFIT/32 Version 3.0, Spectrum Software Associates*, Marlborough, MA 01752, USA, **2000**.
[38] H. Gampp, M. Maeder, C. J. Meyer, A. D. Zuberbühler, *Talanta* **1985**, *32*, 95.
[39] Crystallographic data (excluding structure factors) for H_3*cis*-dap$Cl_3[H_2O$, H_3*trans*-dap$Cl_3 \cdot 0.5H_2O$, [Pt(H*cis*-dap)Cl_4]$Cl \cdot H_2O$, [Pd(H*cis*-dap)$_2$]$(ClO_4)_4 \cdot 2H_2O$, [Co(*cis*-dap)(tach)]-[$ZnCl_4$]$Cl \cdot$EtOH, [Cu(ampy)$_2$]$(ClO_4)_2$, and [Cu(H*cis*-dap)$_2(OH_2)_2](SO_4)_2 \cdot 3.5H_2O - 2x\ H^+ + x\ Cu^{2+}$ (x = 0, 0.08, 0.11) have been deposited with the Cambridge Crystallographic Data Centre as supplementary publication nos. CCDC-161100 to -161109. Copies of the data can be obtained free of charge on application to the CCDC, 12 Union Road, Cambridge CB2 1EZ, U.K. [Fax: (internat.) + 44-1223/336-033; E-mail: deposit@ccdc.cam.ac.uk].
[40] G. M. Sheldrick, *SHELXS-97, Program for Crystal Structure Solution*, Göttingen, **1990**.
[41] G. M. Sheldrick, *SHELXL-97, Program for Crystal Structure Refinement*, Göttingen, **1997**.
[42] H. D. Flack, *Acta Crystallogr., Sect. A* **1983**, *39*, 876.
Received May 9, 2001
[I01165]